PHYSICAL REVIEW LETTERS

VOLUME 6 FEBRUARY 15, 1961 NUMBER 4

INTERACTION OF AN ELECTRON BEAM WITH A FULLY IONIZED PLASMA*

M. A. Allen and G. S. Kino

Microwave Laboratory, W. W. Hansen Laboratories of Physics, Stanford University, Stanford, California

(Received January 30, 1961)

The amplification of microwave signals on an electron beam which passes through a plasma has been observed by Boyd et al.[1] and Bogdanov et al.[2] and discussed in many theoretical papers. However, in the past, because of the nature of the mercury vapor discharge in which these experiments were carried out, it was difficult to obtain a close comparison between theory and experiment. Preliminary experiments using an almost fully ionized thermal cesium plasma have been carried out with encouraging results, and are reported here.

A schematic diagram of the apparatus which was used is shown in Fig. 1. An electron beam passes through a helix on which a microwave signal is induced. The modulated electron beam then passes through a 2.2-cm length of cesium plasma, which is formed from two hot tungsten spiral filaments immersed in cesium vapor. Ions are formed at the filaments by resonance ionization; the electrons are produced by thermionic emission. Both the cesium plasma and the electron beam are confined radially by means of the externally applied magnetic field. The microwave signal on the electron beam is amplified after passing through the plasma and the consequent enhanced modulation is detected on the second helix. Finally, the electron beam is collected on a collector. A water jacket is provided around the plasma region to control the temperature of the cesium vapor, and hence, the vapor pressure and rate of ion emission. Half-wave rectified ac was used on the heaters, and all measurements of interest were carried out during the off-period of the heating cycle. This method of producing a plasma has been shown[3]

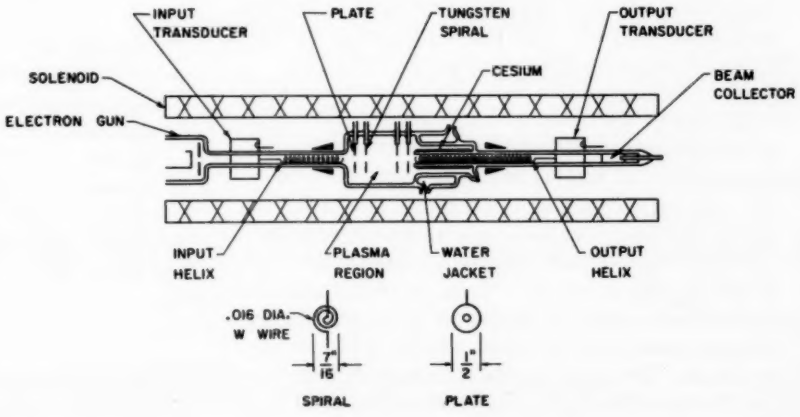

FIG. 1. Cross section of beam-plasma tube shown schematically.

to yield a plasma characterized by a very high percentage of ionization (greater than 10%), with temperatures of the ions and electrons at approximately that of the heater (2300°K). The dominant collision process present is that between electrons and ions.

By measuring the gain of the system, from the input to the output transducers, with the plasma on and the plasma off, it was possible to determine the gain due to the plasma alone. The parameters of the system which could be varied were signal frequency, plasma density, and beam current. Assuming that for a given plasma density the gain was maximum at the plasma frequency, then the maximum gain measured with approximately 1 ma in the beam varied from 10 db at a plasma frequency of 1000 Mc/sec to over 20 db at a plasma frequency of 3000 Mc/sec. At higher plasma frequencies, the gain was so high that the tube oscillated at that value of beam current.

A theoretical analysis has been performed in order to determine the rf gain for a finite electron beam in a finite magnetic field passing through a plasma. By making the assumption of slow waves, it is found that the fields inside and outside the beam have transverse propagation constants T_1 and T_2, respectively, where

$$T_1^2 = -k^2 \frac{1-(\omega_p^2/\omega^2)-[\omega_{pb}^2/(\omega-ku_0)^2]}{1+[\omega_p^2/(\omega_c^2-\omega^2)]+\{\omega_{pb}^2/[\omega_c^2-(\omega-ku_0)^2]\}}, \quad (1)$$

$$T_2^2 = -k \frac{1-(\omega_p^2/\omega^2)}{1+[\omega_p^2/(\omega_c^2-\omega^2)]}, \quad (2)$$

and where u_0 is the electron beam velocity. All fields are assumed to vary as $\exp[i(kz-\omega t)]$; ω_p and ω_{pb} are the plasma frequencies of plasma and beam, respectively; and ω_c is the electron cyclotron frequency for the applied magnetic field. The assumption was made that the plasma frequency of the beam is much less than the cyclotron frequency, and hence, the third term in the denominator of Eq. (1) is negligible. However, with the normal values of magnetic field used in this type of experiment, such an assumption is certainly not justified for the plasma frequency of the plasma electrons. Thus, it is felt that the theoretical results of Bogdanov et al. which rely on this assumption are not applicable to our experiment. The appropriate matching conditions of the fields at the edge of the beam were used to determine that for $\omega_c<\omega<\omega_p$, T_1 is real and T_2 is imaginary. It follows that there should be gain in this range of frequencies which becomes infinite at the plasma frequency. However, because of the nature of the Bessel functions involved, for a finite cylindrical beam the gain approaches infinity not as $(1-\omega_p^2/\omega^2)^{-1/2}$ as in the case of the infinite beam, but only as $\ln(1-\omega_p^2/\omega^2)$. Consequently, any effect in the plasma, such as nonuniformity in the density, finite temperature, or collision losses, causes the measured gain to be finite near $\omega=\omega_p$. Because of the logarithmic behavior of the gain parameter, the actual nature of the loss mechanism need not be known to great quantitative accuracy.

In the range $\omega_p<\omega<(\omega_c^2+\omega_p^2)^{1/2}$ the propagation constant T_2 is real, with the result that, if the beam is finite and small in diameter compared with the wavelength, then there are values of frequency in this range over which the plasma presents an inductive impedance to the beam, and gain would be expected. The nature of the plasma is not known precisely; thus, it can be said only that there is gain within this range, and that its magnitude as a function of frequency does not vary monotonically with frequency but has local maxima and minima. For $\omega>(\omega_c^2+\omega_p^2)^{1/2}$, the predicted gain is zero.

The theoretical curve for gain in the range $\omega_c<\omega<\omega_p$ for a given ω_p is plotted with an experimental curve in Fig. 2. The effect of conduction currents due to cesium collecting on the

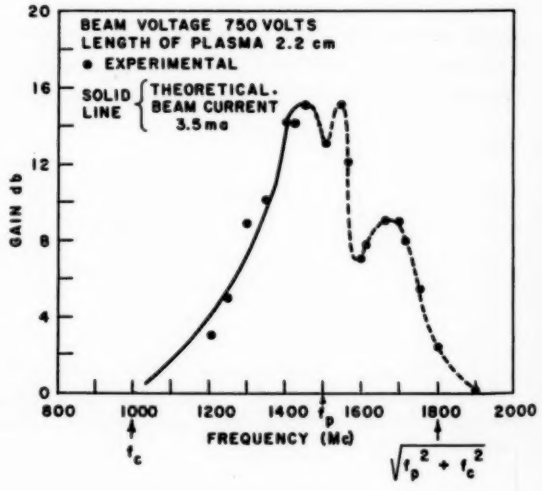

FIG. 2. Gain due to beam-plasma interaction plotted as a function of frequency.

walls of the tube prevented an accurate measurement of beam current being made. The theoretical curves are for an assumed value of 3.5 ma. It is noted that gain is obtained roughly from ω_c to $(\omega_p^2+\omega_c^2)^{1/2}$.

Finally, it is noted that there is an important conclusion to be drawn from finite-beam theory, which in the range $\omega_p<\omega<(\omega_p^2+\omega_c^2)^{1/2}$ gives a propagation constant T_2 which is not only real but may be small. This conclusion is, that it is possible to obtain gain when the fields radiate outwards from the beam, and the wavelength in the radial direction is comparable to the wavelength in free space. Thus, if the plasma ends abruptly, it is possible for such fields to radiate directly into free space. This mechanism might explain how radiation may be emitted from a stellar atmosphere. It may also point to possible methods for detecting rf radiation from a plasma in the laboratory.

Further experiments are being carried out with a modified cesium plasma tube, and it is intended to give a full description of our experimental and theoretical results in a forthcoming paper. The authors are indebted to Sylvania for providing parts of a traveling-wave tube and to Mr. D. L. Masterson for his part in the construction of the experimental tube.

*This research was supported by Air Force Cambridge Research Laboratories, Air Force Research Division, Air Research and Development Command.

[1]G. D. Boyd, L. M. Field, and R. W. Gould, Phys. Rev. 109, 1393 (1958).

[2]E. V. Bogdanov, V. A. Kislov, and Z. S. Chernov, Radiotekh. Elektron. 5, 229 (1960) (translated by Pergamon Press, New York).

[3]M. A. Allen, G. S. Kino, and J. D. Lawson, presented at the Conference on Plasma Physics, American Physical Society, Gatlinburg, November, 1960.

AN ERROR IN THE THERMAL CONDUCTIVITY FOR A FULLY IONIZED GAS

R. W. Vaughan-Williams and F. A. Haas

Atomic Weapons Research Establishment, United Kingdom Atomic Energy Authority, Aldermaston, England

(Received January 17, 1961)

The existence of a discrepancy between the thermal conductivities for a fully ionized gas perpendicular to a magnetic field as calculated by Marshall[1] and by Rosenbluth and Kaufmann[2] has been widely realized for some time. Because of the current interest in transport phenomena and the fact that the presence of such a discrepancy may lead to doubts concerning the validity of the underlying principles of these different calculations, we feel it important to point out the source of this error.

Rosenbluth and Kaufmann compute transport coefficients for large $\omega\tau$, where ω and τ^{-1} denote gyration and collision frequencies, respectively. In particular they find that, assuming $m_i \gg m_e$, the dominant contribution to the thermal conductivity K perpendicular to the magnetic field comes from ion-ion collisions. This result is at variance with the work of Marshall, where in the limit of large $\omega\tau$, all types of collisions contribute significantly to the thermal conductivity. The other transport coefficients are found to be in agreement.

We used the collision integrals listed on page 81 of Marshall[1] to recompute the moments of f_{11} of Rosenbluth and Kaufmann.[2] As expected, the first moment leads to Eq. (10) of Rosenbluth and Kaufmann but the second moment does not give their K. The discrepancy is found to arise through an error in the last collision integral of Marshall.[1] This should read

$$[w_{-2}S_{3/2}^{1}(w_2^2),\ w_{-2}S_{3/2}^{1}(w_2^2)]_2=\sqrt{2}M_1^{1/2}\phi(1-\delta),$$

using Marshall's notation. On inserting this in Eq. (5.4) on page 41, we found that a_1^0 and a_1^1 were unchanged, but that

$$a_2^1=-\tau\left(\frac{2kT}{m_1}\right)^{1/2}\frac{3M_1^{1/2}+0.566+i\omega\tau M_1^{1/2}}{\omega^2\tau^2M_1+9M_1+3.394M_1^{1/2}+0.32}.$$

This leads to

$$\lambda'^{II}=1.25\frac{kn\tau kT}{m_1}\left[\frac{1.866\omega^2\tau^2+0.966}{\omega^4\tau^4+6.282\omega^2\tau^2+0.933}+\frac{3M_1+0.566M_1^{1/2}}{\omega^2\tau^2M_1+9M_1+3.394M_1^{1/2}+0.32}\right],$$

and

$$\lambda'^{III} = 1.25\,\frac{kn\tau kT}{m_1}\left[\frac{\omega\tau M_1}{\omega^2\tau^2 M_1 + 9M_1 + 3.394M_1^{1/2} + 0.32} - \frac{\omega\tau(\omega^2\tau^2 + 1.9)}{\omega^4\tau^4 + 6.282\omega^2\tau^2 + 0.933}\right],$$

corresponding to Eqs. (5.11) and (5.12) on pages 42 and 43, respectively.

In the limit of high fields,

$$\lambda^{II} = \lambda'^{II} = 1.25\,\frac{kn\tau kT}{m_1}\left(\frac{4.866 + 0.566M_1^{-1/2}}{\omega^2\tau^2}\right).$$

This agrees with the result obtained by Rosenbluth and Kaufmann assuming as they do that $m_i \gg m_e$.

[1] W. Marshall, Atomic Energy Research Establishment Report AERE-T/R-2419, 1958 (unpublished).

[2] M. N. Rosenbluth and A. N. Kaufmann, Phys. Rev. 109, 1 (1958).

NUCLEAR PARAMAGNETIC SUSCEPTIBILITY OF LOW-TEMPERATURE He^3 AND THE FLOW PROPERTIES OF SUPERFLUID SYSTEMS OF FERMIONS*

Ronald M. Rockmore
Department of Physics, Brandeis University, Waltham, Massachusetts
(Received January 16, 1961)

It has recently been suggested[1] that a measurement of the magnetic susceptibility furnishes a convenient experiment for the detection of the possible low-temperature phase transition of liquid He^3 to a highly correlated phase. The theoretical basis for this suggestion was provided by the calculation[1] of the temperature behavior of this system in the presence of a uniform magnetic field of arbitrary strength and the temperature-dependent magnetic susceptibility by the method of Bogolyubov et al.[2] using the model of He^3 due to Brueckner et al.[3]

We wish to point out in this note the simple interpretation afforded this calculation by the two-fluid model[4,5] of superfluid many-fermion systems and to indicate how measurement of the magnetic susceptibility together with the moment of inertia of a cylindrical container of the liquid determines the effective mass for flow in the case of an asymmetric gap.[3,5]

The usual restriction to "small fields" (up to the order of 10^5 gauss)[6] permits us to expand Eq. (1) of reference 1 to lowest order in $\beta\kappa$, where $\beta = 1/kT$ and κ is the magnetic field multiplied by μ, the appropriate magneton for He^3, so that one has[7]

$$\chi = \mu^2\beta\sum_{\vec{k}}\{1+\cosh[\beta\Omega(\vec{k})]\}^{-1} = \mu^2 2\beta\sum_{\vec{k}}\frac{\exp[\beta\Omega(\vec{k})]}{\{1+\exp[\beta\Omega(\vec{k})]\}^2}. \quad (1)$$

We may also express χ simply in terms of the statistical factors $f(\vec{k})$ as[4]

$$\chi = \mu^2 2\beta\sum_{\vec{k}} f(\vec{k})[1-f(\vec{k})]. \quad (2)$$

Further, since the summand $f(\vec{k})[1-f(\vec{k})]$ is strongly peaked about the Fermi surface $[k = k_F]$, one may write[8]

$$\chi \simeq (\mu^2/k_F^2)2\beta\sum_{\vec{k}} k^2 f(\vec{k})[1-f(\vec{k})] \quad (3a)$$

$$\simeq 3\mu^2(N_n m/k_F^2) = 3\mu^2 L^3[M_f'(0)/k_F^2], \quad (3b)$$

where $M_f'(0)$ is a linear combination of the effective masses for parallel and perpendicular flow[5] for the case of the asymmetric gap and is the usual effective mass for flow[5] in the symmetric case. N_n is the total number of normal atoms at the temperature T.[9] Finally, on making use of the relation

$$\chi_0 = 3\mu^2(Nm/k_F^2), \quad (4)$$

where χ_0 is the "rigid"[10] or normal value of the susceptibility, we have

$$(\chi/\chi_0) = (N_n/N) = M_f'(0)/nm, \quad (5)$$

where n is the density of atoms.

For purposes of detailed comparison with the work of reference 5, we shall cast the sum $\sum_{\vec{k}} f(\vec{k})[1-f(\vec{k})]$ into its corresponding integral

form, namely,

$$2\beta\sum_{\vec{k}} f(\vec{k})[1-f(\vec{k})]-(L^3/E_F)\tfrac{1}{2}\int_{-1}^{+1}dx F(x) = (L^3/E_F)(K_2+\tfrac{1}{2}K_1), \quad (6)$$

where

$$F(x)=3\beta\int_{|C(x)|}^{\infty} dE[E^2-|C(x)|^2]^{-1/2}Ee^{\beta E}(1+e^{\beta E})^{-2}, \quad (7)$$

and

$$K_2+\tfrac{1}{2}K_1=M_f'(0)/nm; \quad (8)$$

as in reference 5, the positive semidefinite quantities, K_1 and K_2, are, in units of nm, the respective effective masses for parallel and perpendicular flow only. Thus,

$$(\chi/\chi_0)=\tfrac{1}{2}K_1+K_2 \quad (9)$$

Since, as has been noted in reference 5, the corresponding ratio for the moment of inertia, I/I_0, is equal to K_2 for the same asymmetric case, we have

$$K_1=2[(\chi/\chi_0)-(I/I_0)]. \quad (10)$$

Thus the joint measurement of I/I_0 and χ/χ_0 determines the effective mass for flow in the asymmetric case.[5]

It has been noted previously[1] that the lack of good agreement with experiment for very low temperatures indicates that the above result can only be considered as valid near the critical temperature. However, within the region of its validity, a measurement of the magnetic susceptibility should provide a sensitive test of the superfluid character of the system since, by virtue of Eq. (5), it must be considered one of the flow properties of superfluid systems.

---

*This work was supported in part by the Office of Naval Research.

[1]L. H. Nosanow and R. Vasudevan, Phys. Rev. Letters 6, 1 (1961).

[2]N. N. Bogolyubov, D. N. Zubarev, and Yu. A. Tserkovnikov, Doklady Akad. Nauk S.S.S.R. 117, 788 (1957) [translation: Soviet Phys.—Doklady 2, 535 (1957)].

[3]K. A. Brueckner, T. Soda, P. W. Anderson, and P. Morel, Phys. Rev. 118, 1442 (1960).

[4]J. Bardeen, Phys. Rev. Letters 1, 399 (1958); R. M. Rockmore, Phys. Rev. 118, 1645 (1960).

[5]A. E. Glassgold and A. M. Sessler, University of California Radiation Laboratory Report UCRL-9223, 1960 (unpublished). Our notation follows that of this reference closely.

[6]This is also the practical range of interest since, as has been pointed out in reference 1, fields of the order of 10^6 gauss would be needed to observe the critical field even near the critical temperature.

[7]K. Yosida, Phys. Rev. 110, 769 (1958).

[8]The approximation, $\sum_{\vec{k}} c_n(k)f(\vec{k})[1-f(\vec{k})] \cong c_n(k_F) \times\sum_{\vec{k}} f(\vec{k})[1-f(\vec{k})]$, where $c_n(k)$ is a polynomial in k, is quite usual in calculations in the BCS theory [J. Bardeen, L. N. Cooper, and J. R. Schrieffer, Phys. Rev. 108, 1175 (1957)]; see, for example, K. Yosida, Progr. Theoret. Phys. (Kyoto) 21, 731 (1959).

[9]This definition differs slightly from that given in reference 4.

[10]R. M. Rockmore, Phys. Rev. 120, 1933 (1960).

PHONON-PHOTON DOUBLE-QUANTUM TRANSITIONS AS A DETECTOR OF MICROWAVE ULTRASONICS

N. S. Shiren
General Electric Research Laboratory, Schenectady, New York
(Received January 25, 1961)

We have observed double-quantum transitions, in which a microwave photon and an ultrasonic phonon, at different frequencies, are simultaneously absorbed. Orton, Auzins, and Wertz[1] have previously reported similar observations in which photons at two different frequencies were absorbed in a transition between the $S_z = -1$ and $S_z = +1$ levels of Ni^{2+} in MgO at 77°K. Our observations were made at 2°K, on the spin systems of Ni^{2+} and Fe^{2+} in MgO. We are able to confirm the double-quantum nature of the narrow line observed in the spectrum of the latter,[2] as predicted by Orton et al.[1] Further results on phonon-photon double-quantum transitions, and on the interaction of microwave ultrasonics with the two aforementioned ions, will be reported more fully. However, it is the purpose of this Letter to discuss the use of these transitions in the detection of ultrasonic radiation at microwave frequencies, and to report an experimental demonstration of the feasibility of the method.

Detection of microwave ultrasonics by the concomitant saturation of electron spin resonance transitions has been suggested,[3] and its feasibility has been demonstrated under c.w. conditions.[4] As a detector of microsecond pulses, however, the saturation method fails because of the long spin-lattice relaxation times which are characteristic of paramagnetic impurities in solids.

Pulse detection of microwave ultrasonics is presently effected by the inverse of the piezoelectric effect used for ultrasonic generation.[5,6] Because of the small power conversion ($\sim 10^{-4}$ at X band with a cavity $Q = 10^3$) the sensitivity is low. The principal disadvantage, however, is that the output is not always a measure of acoustic intensity, because it is determined by the acoustic wave amplitude, integrated over the face of the piezoelectric crystal. The detected pulse amplitude is consequently extremely sensitive to any deviation of this face from being a constant-phase surface of the wave. Such effects lead to nonexponential decays in pulse echo experiments, and have been discussed in detail by Jacobsen.[5]

Referring to Fig. 1, the double-quantum detection method consists in the measurement of

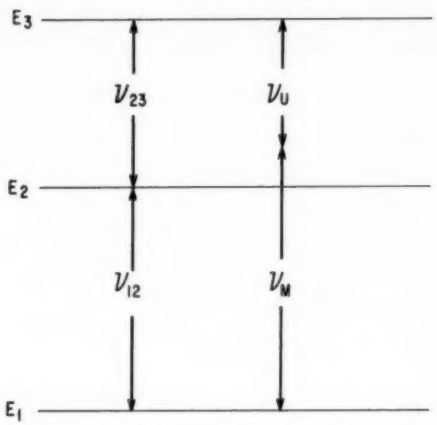

FIG. 1. Energy level scheme showing a possible double-quantum transition for a phonon at frequency ν_U and a photon at ν_M.

microwave power, at frequency ν_M, which is absorbed in double-quantum transitions, at frequency ν_{13}, when ultrasonic power is applied at frequency $\nu_U = \nu_{13} - \nu_M$. Used as a pulse detector, the energy level system is allowed to assume its steady state under the influence of the c.w. microwaves. There is then an increased microwave absorption concurrent with the ultrasonic pulse. The method is capable of detecting very fast pulses because the rise time for absorption is of order T_2, rather than the much larger time, of order T_1, associated with partial saturation at low power levels. The decay time is also $\sim T_2$ since, in the absence of double-quantum transitions, the return of the 1-3 population difference to equilibrium is not observed. Since the double-quantum transition probability is proportional to the product of the two energy densities, the microwave power absorbed is a measure of the acoustic intensity. By using an energy level scheme in which $\nu_{12} > \nu_{23}$, and therefore, for a given transition probability, $\nu_M > \nu_U$, conversion "gain" may be realized, in the sense that the rf power absorbed is greater than the ultrasonic in the ratio ν_M/ν_U.[7]

We have demonstrated double-quantum pulse detection using Fe^{2+} in MgO. As a detector of

ultrasonic energy the ground-state Zeeman transitions of this ion are particularly favorable because of the large spin-phonon coupling. Comparative measurements in the same crystal show that the spin-phonon interaction is $\sim 4\times 10^3$ larger than that for Mn^{2+}, and ~30 larger than for Ni^{2+}. The effective spin is[2] $S=1$ and, as in Ni^{2+},[1] the $S_z=\pm 1$ levels are shifted by local departures from cubic symmetry, leading to an inhomogeneously broadened line, about 400 gauss wide (peak to peak derivative), for the $\Delta M=1$ transitions. The $\Delta M=2$ transition remains sharp, however (6 gauss in our crystals). For a fixed value of ν_M it should therefore be possible to find magnetic field values such that equivalent double-quantum transitions will occur over a range $\nu_U=\nu_M\pm 1000$ Mc/sec, and we have observed them with $\nu_U=\nu_M\pm 300$ Mc/sec. Used as a detector, the need for tunable receiving and/or generating circuits is therefore eliminated.

The experimental geometry was similar to that previously reported.[4] A 1.75-cm long x-cut quartz crystal transducer was bonded to an MgO crystal 1.4 cm in length along a cubic axis. Both crystals were 3 mm in diameter. The end faces of the quartz and the bonding face of the MgO were optically polished. The back end of the latter was rough cut. The MgO crystal extended across the short dimension of a full-wave rectangular cavity resonator tuned to 9.2 kMc/sec, and the bonded face of the crystal lay just inside the cavity. The back end extended outside the opposite cavity wall. 0.5-μsec ultrasonic pulses were generated at the opposite end of the quartz by standard techniques.[5] Video detection of the microwave absorption was effected by a pair of MA408A crystals.

The observed double-quantum pulses are shown on the lower trace of Fig. 2, for a 50-watt ultrasonic drive pulse at 9.45 kMc/sec, and 30-mw c.w. microwaves at 9.21 kMc/sec. The upper trace is the piezoelectrically detected output at the generating end of the quartz. The transmitter pulse is observed first, followed by echoes in the quartz. No echoes from the back end of the MgO are seen, due to the rough surface and strong absorption by Fe^{2+} $\Delta M=1$ transitions. The double-quantum pulses appear halfway (measured at the start of the rise) between the echoes in the upper trace, since they are observed at the time of transmission through the bond. Their rise and decay times are determined by the ultrasonic pulse length, i.e., by the time taken for all the energy to be within the

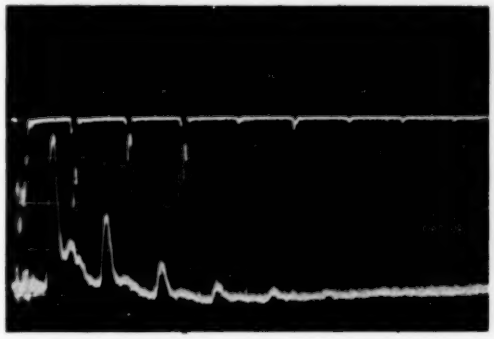

FIG. 2. Lower trace: double-quantum signal after crystal video detection, for ultrasonic frequency 240 Mc/sec higher than the rf. Upper trace: piezoelectric signal after superheterodyne detection. The time between successive echoes is 6.2 μsec. The initial wiggles in the double-quantum output, which appear simultaneously with the direct magnetron pulse in the upper trace, are due to electrical pickup from the pulser. The shape of the piezoelectric echoes is due to double pulsing and frequency modulation of the magnetron.

cavity. The total observed double-quantum pulse width is thus the sum of this rise time and the transmission time through the cavity. The two smaller pulses following each large one are consecutive reflections from the back and front faces of the MgO. They are observed despite the loss of a coherent wave front (by reflection at the rough surface) which partially destroys these echoes in the piezoelectric detector. Also, the nonexponential decay of the echo pattern in the upper trace, which is caused by a similar effect mentioned earlier, is not observed in the double-quantum echo pattern which does decay exponentially. The background level is believed to be an enhanced rf absorption by those spins for which $\nu_M=\nu_{12}$ and $\nu_U=\nu_{23}$, due to partial saturation of the 2-3 $\Delta M=1$ transition by the ultrasonics. Its decay time, which should be $\sim T_1$, is shortened by the amplifier response.

It will be noted that the detection sensitivity is lower than for the piezoelectric output with superheterodyne post detection. However, it can be improved by using higher rf measurement power, better video amplification (noise in the lower trace is all amplifier noise), and particularly by using higher Fe^{2+} concentrations. In our crystals the concentration is ~0.02%, and the effective concentration for the narrow double-quantum transition is about 1% of this. The crystal length

should be smaller than the one we used in order to obtain the best ratio of pulse amplitude to total energy absorption. The optimum length is one just long enough to completely contain the ultrasonic pulse so that the output reaches its full amplitude. Results on optimization of the detector, together with a detailed analysis, will be reported at a later date.

The advent of an intensity (rather than integrated amplitude) detector will facilitate experiments which have not heretofore been possible. As an example, it will allow observation of incoherent acoustic energy, important in the study of boundary scattering. Absolute ultrasonic energy measurements are also possible, since the microwave power absorbed may be calibrated if the transition probability and numbers of spins are known.

It is a pleasure to acknowledge discussions on various aspects of this work with Dr. T. G. Castner, Dr. E. H. Jacobsen, Dr. E. B. Tucker, and Dr. G. D. Watkins. T. G. Kazyaka aided in all the experimental work.

[1]J. W. Orton, P. Auzins, and J. E. Wertz, Phys. Rev. Letters 4, 128 (1960).

[2]W. Low, Phys. Rev. 118, 1130 (1960).

[3]C. Kittel, Phys. Rev. Letters 1, 5 (1958).

[4]E. H. Jacobsen, N. S. Shiren, and E. B. Tucker, Phys. Rev. Letters 3, 81 (1959).

[5]E. H. Jacobsen, Quantum Electronics (Columbia University Press, New York, 1960), pp. 468-482.

[6]H. E. Bömmel and W. Dransfeld, Phys. Rev. 117, 1245 (1960).

[7]E. H. Jacobsen has pointed out that the inverse, in a properly chosen energy level scheme such that $\nu_U >> \nu_M$, allows detection of very high frequency phonons by low-frequency rf.

SURFACE STATES ON CLEAVED SILICON*

D. R. Palmer, S. Roy Morrison, and C. E. Dauenbaugh
Honeywell Research Center, Hopkins, Minnesota
(Received November 11, 1960)

Measurements of surface band structure on silicon (111) surfaces cleaved in vacuum (10^{-7} to 10^{-10} mm) have been made using both the field-effect approach[1,2] and the channel method of Statz and his co-workers.[3]

In the field-effect measurements the portion cleaved off the sample was used as the field plate, and measurements were taken with fields up to 10^4 volts/cm. The field-effect measurements show a slightly *n*-type surface on both *p*- and *n*-type bulk material, of field-effect mobility of about 50 cm^2/v sec. The surface is extremely insensitive to oxygen admission, with up to atmospheric oxygen pressure producing negligible change in field effect, and no sudden changes of conductance with increasing pressure. The latter measurement is unreliable over long periods of time due to temperature drifts. Because of this insensitivity to ambient, the measurement cannot distinguish between a strongly *n*-type surface with a high density of states or a surface which is almost intrinsic.

To discriminate between the above techniques, the channel method of Statz was employed. Samples were made by diffusing phosphorus into 80-ohm-cm *p*-type silicon to form *npn* units and by diffusing boron into 20-ohm-cm *n*-type silicon to form *pnp* units. The "base" width was 0.04 inch. By cleaving so as to leave the junctions intersecting a cleaved surface, we were able to make measurements of the channel conductance, if any, caused by the cleaved surface. In neither the *npn* nor the *pnp* case was the conductivity of the cleaved surface greater than 10^{-2} μmho/square at 1.5 volts bias, indicating there was no channel (inversion layer) present. This can be compared, for example, with a conductance of about 90 μmho/square as measured by the Statz technique on a cleaved surface of 5-ohm-cm *n*-type germanium (*pnp* configuration).

Thus we conclude that the dominant surface states are near the center of the gap with a freshly cleaved silicon surface, if we assume the surface state structure independent of the bulk type.

This result is in disagreement with work on ion-bombarded surfaces, where Law[4] has found a *p*-type accumulation layer on *p*-type silicon after bombardment and annealing and has found that the surface becomes *n*-type after bombardment with 1000-volt argon ions. He has also stated without reference that earlier work showed

a p-type surface on n-type silicon. Dillon and Farnsworth[5] have concluded via work function and photoelectric threshold measurements that a degenerate p-type layer is found on a silicon surface cleaned by ion bombardment and annealing.

*This research was supported in part by the U. S. Air Force under a contract monitored by the Air Force Office of Scientific Research of the Air Research and Development Command.

[1]D. R. Palmer and C. E. Dauenbaugh, Bull. Am. Phys. Soc. 3, 138 (1958).

[2]D. R. Palmer, S. R. Morrison, and C. E. Dauenbaugh, Semiconductor Surfaces (Pergamon Press, New York, 1960), p. 27.

[3]H. Statz, G. A. DeMars, L. Davis, Jr., and A. Adams, Jr., Semiconductor Surface Physics (University of Pennsylvania Press, Philadelphia, Pennsylvania, 1957), p. 139.

[4]J. T. Law, Semiconductor Surfaces (Pergamon Press, New York, 1960), p. 17.

[5]J. A. Dillon and H. E. Farnsworth, J. Appl. Phys. 29, 1195 (1958).

STORED ENERGY RELEASE BELOW 80°K IN DEUTERON-IRRADIATED COPPER*

A. V. Granato† and T. G. Nilan‡
Department of Physics, University of Illinois, Urbana, Illinois
(Received December 22, 1960)

Experiments by Blewitt, Coltman, and Klabunde[1] on neutron-irradiated copper have shown that the energy released during annealing in the vicinity of 40°K, designated Stage I, is 1.6 calories/g per μohm cm of resistivity which anneals. This value is anomalously low and leads to doubts as to whether or not interstitial-vacancy mutual annihilation can be the recovery mechanism. Further, since the annealing observed in deuteron-irradiated copper is in some ways similar to that found in neutron damage, the doubt attaches also to the deuteron results. An experiment was therefore performed to measure the energy released after 11-Mev deuteron irradiation.

For the measurement, a specially designed differential calorimeter was constructed in which it was possible to measure all heat leaks as a function of temperature. This was required since the total anticipated energy release is small, and leaks are a significant part of the total effect. The magnitude of the energy released was limited on the one hand by the smallness of the specimen and on the other hand by the necessity to keep the total stored energy released per gram per temperature interval considerably less than the specific heat to avoid making the specimen thermally unstable.[2] The size of the specimen was limited by the deuteron beam size and range. The above requirements were met by using a $\frac{1}{2}$-g specimen,[3] 5×10^{-3} in. thick, in deuteron fluxes several times smaller than those which have been used in previous radiation-damage measurements and a relatively fast annealing rate of about 2°K/min. The heat leaks were minimized to an extent consistent with the requirement of reproducibility by using high thermal resistivity Advance-Chromel P thermocouple wires and pressures less than 10^{-5} mm Hg in the experimental volume.

Departures of the differential system from perfect symmetry were taken into account by use of a separate background annealing run, in which the specimen in an unirradiated state and its symmetric dummy were heated to 80°K, and subsequently cooled. This run was also used to measure the heat leaks and the specific heat of the specimen as a function of temperature. The important influence of the rapidly varying specific heat on the results as well as other aspects of the measurement will be discussed in detail in a later publication. A continuous recording of the output of a differential thermocouple between the copper foils was made during the anneal. From this recording, calculations could be made at temperatures as closely spaced as desired.

The results are shown in Fig. 1, where the energy released per gram per unit temperature is plotted in millicalories per gram-°K as a function of the annealing absolute temperature. Two irradiations and subsequent anneals were made: Run I to an integrated flux of 8.25×10^{15} deuterons/cm^2 and Run II to 2.89×10^{15} deuterons/cm^2. The part of the curves below 27°K is blurred by a complication due to experimental difficulties in fixing the starting point of the annealing, and

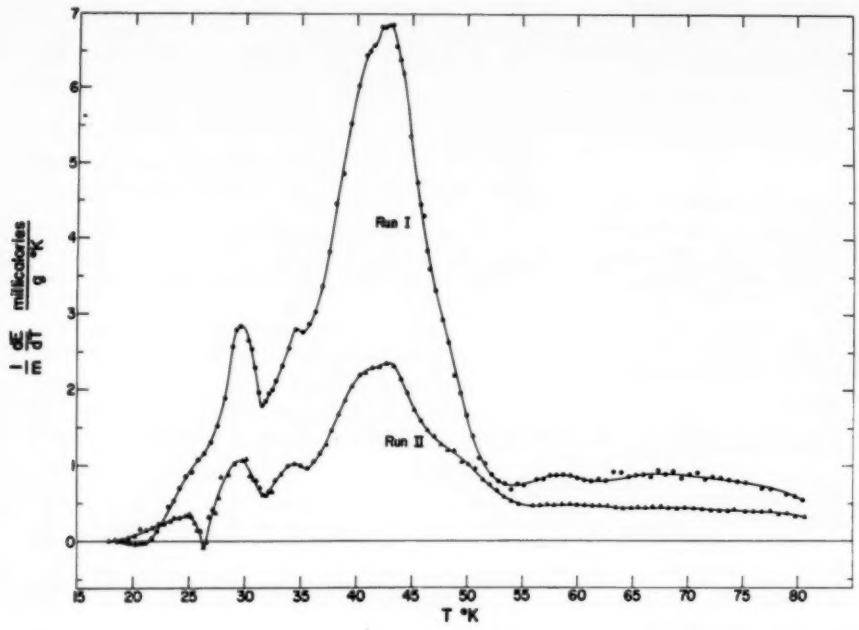

FIG. 1. Stored energy release in deuteron-irradiated copper. ● – Run I; $\Phi = 8.25 \times 10^{15}$ deuterons/cm^2; $(E/m)_{25°-55°K} = 92.8$ millicalories/gram. ▲ – Run II; $\Phi = 2.89 \times 10^{15}$ deuterons/cm^2; $(E/m)_{25-55°K} = 35.3$ millicalories/gram.

should be ignored at this time.[4] Between 27 and 55°K there are three peaks. In Run II, the large peak has a pronounced high-temperature shoulder at about 50°K. Between 55 and 80°K there is a more or less structureless additional annealing. When the two runs are normalized to the same total flux, the three main peaks are in close agreement as to size and shape, except for the high-temperature side of the large peak.

In Fig. 1, one finds 92.8 and 35.3 millicalories/g as the total energy released between 25 and 55°K, for Run I and Run II, respectively. To facilitate computations and comparison with the earlier deuteron experiments, these results were normalized to a flux of 10^{17} deuterons/cm^2 and a deuteron energy in the foil of 10 Mev. An 11-Mev deuteron has an average energy in 5 mils of copper of 7.04 Mev. The average of the normalized energy release is then 0.83 cal/g. The claimed accuracy has not yet been fixed, although it is expected to be of the order of 10% or less. To relate this energy release to previously determined experimental observations of resistivity and volume changes, we use the resistance increment given by Cooper, Koehler, and Marx,[5] the fractional recovery found in Stage I by Simmons and Balluffi[6] (less the lowest temperature peak) of 54%, and the volume change found by Simmons and Balluffi and Vook and Wert.[7] The resulting experimental ratios normalized to the same deuteron flux and energy are $[\Delta(E/m)]/\Delta\rho = 7.1$ cal/g μohm cm and $(\Delta E/\Delta V) = 4.2$ ev per atomic volume change. If the energy per Frenkel pair (F.P.) is assumed to be 5.0 ev, these figures would lead to a resistivity of 2.6 μohm cm per 1% F.P. and 1.2 atomic volumes per F.P. Meechan and Sosin[8] recently found a value of 5.4 for $[\Delta(E/m)]/\Delta\rho$ in a measurement of the stored energy released at low temperatures after electron irradiation. The sensitivity available to them was less than that used here, and they indicated that their results could well be higher.

When the curves of Fig. 1 are compared with the recent isothermal resistivity measurements at higher doses of Magnuson, Palmer, and Koehler,[9] one finds a close agreement for Run I for the peak structure in Stage I. The peak positions in the present work are shifted somewhat to higher temperatures because of the higher heating rate. The peak shapes are better defined in the energy measurements because the data are essentially continuous. This better definition shows structure in the large recovery peak at 42°K, present in both runs. Although the additional continuous annealing above Stage I (above 55°K) is not observed in the resistivity measurements, an additional annealing in this range is found in the lattice-parameter measurements of Simmons and Balluffi.

When the results are compared with those of Corbett, Smith, and Walker[10] for electron irradiation, one sees again agreement as to number and location of peaks in Stage I, although little or no Stage II is observed in electron irradiation. Corbett, Smith, and Walker and Koehler, Seitz, and Simmons[11] have interpreted peaks *A* (below 20°K), *B* (~29°K), and *C* (~34°K) as close interstitial-vacancy pairs, peak *D* (~43°K) as correlated recombination of an interstitial with its own vacancy, and the concentration-dependent peak *E* (~50°K in Run II) as uncorrelated long-range interstitial recombination. Our results support this interpretation of peaks *B*, *C*, and *E*, and, in addition, permit further conclusions to be drawn with regard to them and to peak *D*. The close-pair peaks of Corbett, Smith, and Walker have half-widths very close (~2°K) to the natural half-widths which are to be expected for a single discrete activation energy and low doses, according to calculations we have made which will be presented later. This analysis, which takes into account the thermal instability mentioned earlier,[2] shows that the half-width of the energy release curve is increased when the energy release per degree is a sizable fraction of the specific heat. This condition is readily obtained at low temperatures and typical deuteron damage levels. The half-widths we find for deuteron irradiation are somewhat wider than those which should occur for a unique activation energy (see, for example, peak *B*). This can also be taken as evidence for clusters in deuteron damage since the resulting strain fields in a cluster could broaden out a unique activation energy somewhat. In addition, one finds that peak *D* is far too wide for a unique activation energy but can be interpreted as a superposition of many close pairs with activation energies closely spaced and approaching a limit which is equal to that associated with the freely-migrating interstitial of peak *E*. This conclusion is supported by the evidence of structure in peak *D*. Thus the large width of peak *D*, plus the fact that peak *D* has structure, leads us automatically to the close-pair model of radiation damage at low temperatures.

The authors wish to express their thanks to Professor J. S. Koehler for his continuous advice and help in carrying through the experiment. The help of Mr. R. Seigel, Professor R. Coleman, Dr. M. Garfinkel, Professor R. O. Simmons, and Dr. J. Bredt is gratefully acknowledged. They thank the members of the Nuclear Radiation Laboratory under Professor J. S. Allen, Professor S. Chatterjee, and Mr. L. Ernest and the Liquid Helium Service under Professor D. E. Mapother for their generous assistance. Also, they are indebted to Mr. F. Witt for much useful advice and help, particularly on the construction of the calorimeter.

---

*This research was supported by the U. S. Atomic Energy Commission.

†Now at the Institut für Metallphysik, Aachen, Germany.

‡This author wishes to express his gratitude to the Applied Research Laboratory of the United States Steel Corporation for their personal support.

[1]T. H. Blewitt, R. R. Coltman, and C. E. Klabunde, Phys. Rev. Letters 3, 132 (1959).

[2]This instability is similar in origin to the "Wigner catastrophe" found in graphite moderators of nuclear reactors after long irradiation.

[3]Actually only 40% of the specimen could be irradiated because of the manner in which the specimen was mounted.

[4]It has been expected that the heating of the specimen by the beam would be great enough to wipe out the annealing stage below 26°K. This did not occur completely; hence the lowest peak is distorted.

[5]H. G. Cooper, J. S. Koehler, and J. W. Marx, Phys. Rev. 94, 496 (1954).

[6]R. O. Simmons and R. W. Balluffi, Phys. Rev. 109, 1142 (1958).

[7]R. Vook and C. Wert, Phys. Rev. 109, 1529 (1958).

[8]C. J. Meechan and A. Sosin, Phys. Rev. 113, 422 (1959).

[9]G. D. Magnuson, W. Palmer, and J. S. Koehler, Phys. Rev. 109, 1990 (1958).

[10]J. W. Corbett, R. B. Smith, and R. M. Walker, Phys. Rev. 114, 1452 (1959).

[11]J. S. Koehler, F. Seitz, and R. O. Simmons, Atomic Energy Commission Report AECU-3684, 1958 (unpublished).

RESTORATION OF STABILITY IN FERROMAGNETIC RESONANCE

H. Suhl
Physics Department, University of California, La Jolla, California
(Received January 30, 1961)

As has long been recognized,[1-5] ferromagnetic resonance is subject to instability when the radio-frequency signal exceeds a certain threshold value. In the more common type of instability, pairs of spin waves with equal and opposite momenta grow far beyond their normal, thermal equilibrium amplitudes at the expense of the uniform precessional motion induced by the signal field. In this paper we show how, by rather simple means, this threshold may be substantially raised. The method is reminiscent (in the time domain) of the alternating gradient stabilization (in the space domain) of charged beams. Studies of large motions of the magnetization, which have proved very fruitful in nuclear resonance, may now become possible.

The method we propose is based on the following observations. The natural frequency of the spin-wave pair prone to unstable growth stands in a very sensitive relation to the signal frequency, as is obvious from energy conservation requirements. If now the natural frequency of these spin waves is varied in time, no pair of waves will satisfy the necessary frequency relation for longer than an instant, and this must inevitably cause an increase in the threshold signal. The extent to which this principle is borne out in practice is described in another Letter in this issue.[6]

In standard form, the equations of motion for a potentially unstable spin-wave pair of wave numbers $(\vec{k}, -\vec{k})$ may be written

$$\dot{a}_{\vec{k}} = i\omega_{\vec{k}} a_{\vec{k}} + P_{\vec{k}} a_0^{\,n} a_{-\vec{k}}^{\,*} - \eta_{\vec{k}} a_{\vec{k}},$$

$$\dot{a}_{-\vec{k}}^{\,*} = -i\omega_{\vec{k}} a_{-\vec{k}}^{\,*} + P_{\vec{k}}^{\,*} (a_0^{\,*})^n a_{\vec{k}} - \eta_{\vec{k}} a_{-\vec{k}}^{\,*}. \qquad (1)$$

Here $\omega_{\vec{k}}$ is the natural frequency of the spin wave; $a_{\vec{k}}$ and a_0, respectively, are the amplitudes of the spin wave and of the uniform precession. $P_{\vec{k}}$ is a coefficient measuring the strength of the nonlinear coupling. $\eta_{\vec{k}}$ is a phenomenological loss constant for the spin wave. n is a positive integer measuring the order of the nonlinear coupling. Only the cases $n = 1, 2$ have been observed so far. Equations (1) predict exponential growth of the spin-wave pair when

$$|a_0|^n > \eta_{\vec{k}} / P_{\vec{k}}, \qquad (2)$$

provided the frequency ω which drives a_0 is such that

$$\omega = 2\omega_{\vec{k}}/n. \qquad (3)$$

Equation (3) determines a surface in k space, upon which the right-hand side of Eq. (2) is minimized, to find which spin wave consistent with (3) goes unstable first, and at what minimum power.

We now impose a slow sinusoidal modulation of frequency ν and amplitude h on the applied steady field. ν will ordinarily be much less than ω, or $\omega_{\vec{k}}$. So long as this is so, the equations of motion remain very nearly the same as (1), except that the constants therein become sinusoidal functions of the time. For reasons which will become clear, the time variation of $P_{\vec{k}}$ may be neglected. The time variation of a_0 will be important only in the case $n = 2$, when the modulation will tend to sweep the field clear through the resonance line, and then only if the modulating field exceeds the linewidth. In this paper we neglect the time variation of a_0 which is easily taken into account, if desired.

To first order in the modulating field h, we have, for the time-dependent spin-wave frequency,

$$\omega_{\vec{k}}' = \omega_{\vec{k}} + (\partial\omega_{\vec{k}}/\partial H) h \cos\nu t. \qquad (4)$$

A change of variables,

$$a_{\vec{k}} = A_{\vec{k}} \exp\{i[\omega_{\vec{k}} t + (h\,\partial\omega_{\vec{k}}/\nu\,\partial H)\sin\nu t] - \eta_{\vec{k}} t\},$$

$$A_0 = a_0 \exp(i\omega t),$$

renders Eq. (1) of the form

$$\dot{A}_{\vec{k}} = P_{\vec{k}} A_0^{\,n} \exp[i(n\omega - 2\omega_{\vec{k}})t - 2i(f/\nu)\sin\nu t] A_{-\vec{k}}^{\,*}, \qquad (5)$$

together with the "adjoint" equation. Here we have defined an additional frequency, $f = h\,\partial\omega_{\vec{k}}/\partial H$. Let us now confine further discussion to the case $n = 1$, for definiteness, and also because the neglect of the time variation of $A_0 = |a_0|$ is then most certainly justified. The condition most favorable

to instability is then, provisionally at any rate, $\omega_{\vec{k}} = \omega/2$. For spin waves satisfying this condition, we have

$$\dot{A}_{\vec{k}} = A_0 P_{\vec{k}} A_{-\vec{k}}^* \exp(-2if/\nu) \sin\nu t$$
$$= A_0 P_{\vec{k}} A_{-\vec{k}}^* \sum_{m=-\infty}^{+\infty} J_m(2f/\nu) \exp(-im\nu t). \quad (6)$$

The right-hand side of this equation consists of one secular term and a series of nonsecular terms. In the crudest approximation only the secular term contributes to the instability phenomenon. In this approximation, then, we retain only the term with the secular coefficient, $P_{\vec{k}} J_0$. Instead of the instability criterion (2), we then have

$$A_0 = \eta_{\vec{k}} / P_{\vec{k}} J_0(2f/\nu).$$

Hence if the modulating field amplitude and the modulating frequency are chosen so that the argument of the zero-order Bessel function in this expression is equal to one of its zeroes, the threshold becomes theoretically infinite. In a more refined approximation the threshold is, generally, finite. The solution of (5) and its adjoint will have the form

$$A_{\vec{k}} = e^{\lambda t} \sum_{r=-\infty}^{+\infty} B_r e^{ir\nu t},$$

where the B's in the summation are constants, satisfying the equation

$$B_n = A_0^2 |P_{\vec{k}}|^2 \sum_{m=-\infty}^{+\infty} K(n,m;\lambda) B_m, \quad (7)$$

where

$$K(n,m;\lambda) = \sum_{r=-\infty}^{+\infty} J_{n-r} J_{r-m} / (\lambda + ir\nu)(\lambda + in\nu),$$

the argument of the two Bessel functions in this expression being the same as above. Since Eq. (7) leads to a very complicated infinite determinant relation for λ, we instead discuss a completely soluble case: that of square-wave modulation. For the first half-period, $T/2$, we assume that the frequency condition $\omega_{\vec{k}} = \omega/2$ is satisfied exactly; for the second half-period we assume a deviation f. Then the equation for A [$= a_{\vec{k}} \exp(i\omega_{\vec{k}} t)$] becomes

$$\dot{A} = A_0 P A^*, \qquad (0 < t < \tfrac{1}{2}T)$$
$$\dot{A} = ifA + A_0 P A^*, \qquad (\tfrac{1}{2}T < t < T) \quad (8)$$

where the $\vec{k}$ subscripts have been omitted.

Equations (8) are solved in the two half-periods and fitted together at $\frac{1}{2}T$ by the requirement that A, A^* are continuous there. Next, a linear combination of $A(T)$ and $A^*(T)$ is formed in such a way that it is proportional, with a factor of proportionality $\exp\lambda T$, to the same linear combination of $A(0)$ and $A^*(0)$. Stability is achieved if $\lambda < \eta_{\vec{k}}$. Some algebra shows that λ is given by

$$\lambda T = \cosh^{-1}[\cosh\tfrac{1}{2}P_1 T \cosh\tfrac{1}{2}\Omega T + (P_1/\Omega) \sinh\tfrac{1}{2}P_1 T \sinh\tfrac{1}{2}\Omega T],$$

where $\Omega^2 = P_1^2 - f^2$ and where $P_1 = A_0 P$. A particularly interesting condition arises when the argument of the inverse hyperbolic cosine is less than unity. Then λ is imaginary and the system is stable, no matter how small $\eta_{\vec{k}}$. It is easily verified that this condition of absolute stability is satisfied only when Ω is imaginary, i.e., when the depth of modulation f exceeds $A_0 P$. This is, of course, to be expected from the general threshold conditions (see references 1-5) for spin waves failing to satisfy the frequency condition. For modulation frequencies much smaller than $A_0 P$ the absolute stability criterion is particularly easily interpreted. First, for general T, absolute stability is achieved when

$$|\cos(\tfrac{1}{2}\Omega' T - \phi)| \leq R^{-1},$$

where

$$R = [\cosh^2(\tfrac{1}{2}P_1 T) + (P_1^2/\Omega'^2) \sinh^2(\tfrac{1}{2}P_1 T)]^{1/2},$$

$$\Omega'^2 = f^2 - P_1^2, \quad (>0)$$

and

$$\tan\phi = (P_1/\Omega') \tanh(\tfrac{1}{2}P_1 T).$$

For large $P_1 T$ we thus require

$$\tfrac{1}{2}\Omega' T > \phi = (n + \tfrac{1}{2})\pi.$$

The interpretation is that for large $P_1 T$ only the growing solution of (8) is of importance at the end of the first half-cycle. For $f > P_1$, the solution in the second half-cycle is purely oscillatory and, by judicious choice of T, etc., can always be made to vanish at T, no matter how large its amplitude was at $\frac{1}{2}T$.

All the results in this note apply to instabilities due to parallel pumping as well. It is necessary only to redefine A_0 as the pumping field amplitude itself.

Stabilization can also be achieved by modulating the signal frequency, but this will gener-

ally be less convenient.

[1]P. W. Anderson and H. Suhl, Phys. Rev. 100, 1788 (1955).
[2]H. Suhl, Phys. Rev. 101, 1937 (1956).
[3]H. Suhl, J. Phys. Chem. Solids 1, 209 (1957).
[4]E. Schlömann, J. J. Green, and U. Milano, J. Appl. Phys. 31, 386S (1960).
[5]F. R. Morgenthaler, J. Appl. Phys. 31, 95S (1960).
[6]T. S. Hartwick, E. Peressini, and M. T. Weiss, following Letter [Phys. Rev. Letters 6, 176 (1961)].

SUPPRESSION OF SUBSIDIARY ABSORPTION IN FERRITES BY MODULATION TECHNIQUES

T. S. Hartwick, E. R. Peressini, and M. T. Weiss
Components Division, Hughes Aircraft Company, Culver City, California
(Received January 30, 1961)

In the preceding paper,[1] Suhl has shown theoretically that the threshold power for subsidiary absorption in ferrites can be increased by superimposing on the dc magnetic field, H_{dc}, a small ac modulation, H_m. Experiments have been performed which confirm the above prediction and show that subsidiary absorption can indeed be suppressed at power levels as high as 10 db above the threshold power.

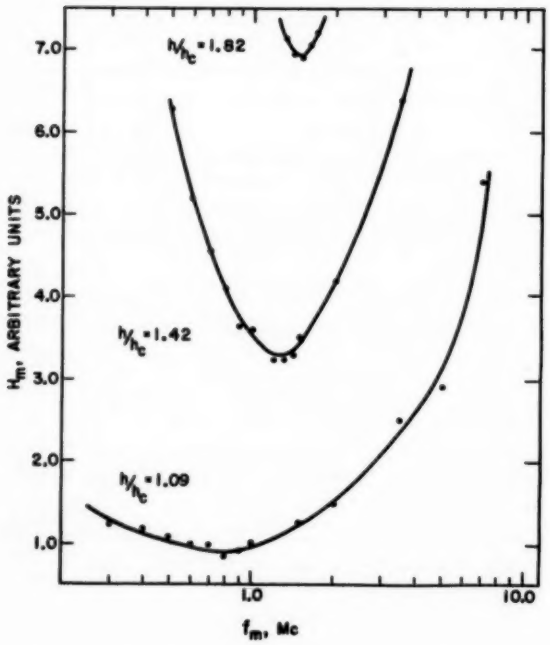

FIG. 1. The minimum modulating field, H_m, required to suppress perpendicular pumped subsidiary resonance as a function of the modulation frequency for various microwave fields.

The experiments were performed on an yttrium iron garnet (YIG) sphere 0.059 inch in diameter with a uniform precession linewidth of 1.2 oe. The sphere was placed near the wall of a cavity resonant at 9250 Mc/sec. Eddy current losses were minimized by using a cavity wall 0.002 mm thick and thus an external modulating coil was suitable. In Fig. 1 a plot is shown of the relative amplitude of H_m required to suppress subsidiary resonance for various values of microwave field, h. For these data h was oriented perpendicular

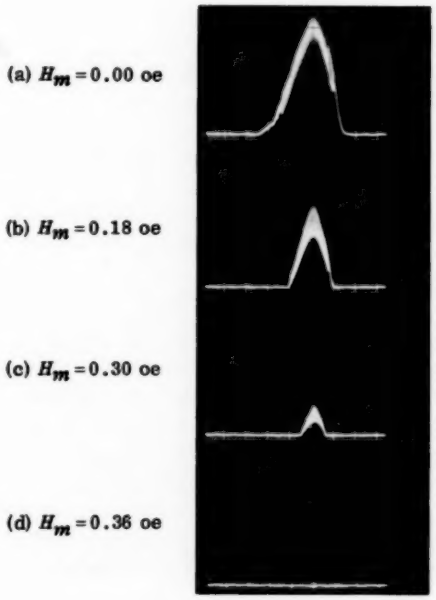

FIG. 2. Absorption is recorded on the vertical axis as H_{dc} is traversed through parallel pumped subsidiary resonance. Horizontal scale is 20 oe/cm. The modulating field is increased from trace (a) through trace (d).

to H_{dc} which was set to 2054 oe, the subsidiary resonance peak. The results show that the optimum modulation frequency is about 0.8 Mc/sec for a microwave field near the threshold field, h_c. Furthermore, it is evident that H_m is quite sensitive to changes in either modulation frequency or microwave field. These results are in general agreement with the Suhl theory although a detailed comparison cannot as yet be made.

The above Suhl theory can, of course, be extended to the parallel pumped case where the microwave magnetic field is parallel to the dc field. Figure 2 shows the results obtained for this parallel pumped condition. In Fig. 2(a) an oscilloscope trace shows the subsidiary absorption as a function of H_{dc} with no modulation applied. The noisy absorption is due to the relaxation oscillations which usually accompany subsidiary resonance.[2] As the modulation field amplitude is slowly increased, the subsidiary absorption gradually becomes suppressed as shown in the succeeding traces 2(b), 2(c), and 2(d). For this microwave field ($h/h_c = 1.26$) a modulating field of 0.36 oe is required for complete suppression. The optimum modulating frequency is 0.25 Mc/sec as compared to the 0.8-Mc/sec frequency for the perpendicular pumped case of Fig. 1. At power levels of 5 db or more above threshold the disappearance of the absorption with increasing modulation amplitude takes place in a discontinuous manner and will be described in detail in a forthcoming paper. The application of these results as a tool to explore the spin-wave spectrum and to various microwave devices will also be discussed.

---

[1]H. Suhl, preceding Letter [Phys. Rev. Letters 6, 174 (1961)].

[2]T. S. Hartwick, E. R. Peressini, and M. T. Weiss, Sixth Annual Conference on Magnetism and Magnetic Materials, New York, 1960 (to be published).

OSCILLATORY MAGNETORESISTANCE IN n-TYPE PbTe

C. D. Kuglin, M. R. Ellett, and K. F. Cuff
Lockheed Research Laboratories, Palo Alto, California
(Received January 6, 1961)

Distinct oscillations of the transverse magnetoresistance of three oriented single crystals of n-type PbTe in dc magnetic fields have been observed. These results confirm the existence of a multivalley band structure having prolate energy ellipsoids oriented along the ⟨111⟩ crystalline axes.[1,2] It is further established that there are four ellipsoids, thus locating the energy minima at the zone edge. The temperature dependence of the oscillatory amplitudes yields a value for the cyclotron mass m_e^* and, in addition, the transverse and longitudinal effective masses are calculated. A recent note,[3] describing the behavior of the transverse magnetoresistance in pulsed fields in an n-type PbTe crystal, has given indications of oscillatory effects. However, the measurements, showing a single minimum, were not interpreted in terms of a possible model for the band structure.

The bulk of our measurements were made on a [110]-oriented sample having a carrier concentration n of $3.45\times10^{17}/cm^3$ and a Hall mobility of 1.2×10^5 cm^2/volt-sec at 1.7°K. With the current along the [110] direction, measurements as shown in Fig. 1 were obtained with magnetic fields up to 26.5 kgauss in the [001] and [1$\bar{1}$0] directions at 1.7 and 4.2°K. Measurements made on additional [110] and [100] samples having dif-

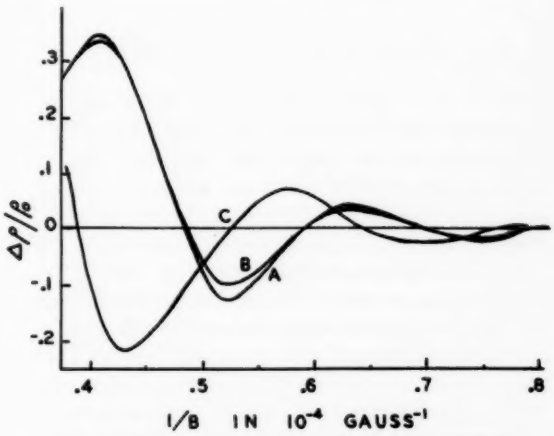

FIG. 1. Oscillatory component of the transverse magnetoresistance for current along [110]; curve A: B_{001} at 1.7°K; curve B: B_{001} at 4.2°K; curve C: $B_{1\bar{1}0}$ at 1.7°K. ρ_0 is the zero-field resistivity.

ferent carrier concentrations yielded oscillatory effects of lower amplitudes but leading to results in agreement with the data presented. Oscillatory effects in the longitudinal direction were not resolved in these samples, the amplitudes being at least an order of magnitude smaller than the transverse effects. In all cases, magnetoresistance and Hall voltage measurements were made using standard four-probe techniques. Data were taken for all combinations of current and magnetic field directions on two sides of the crystal and the results averaged. The Hall voltage and the magnetoresistance above 1 kgauss were linear functions of the magnetic field with a small oscillatory component superimposed. The oscillatory part was obtained by biasing out the linear term with a signal from a rotating-coil gaussmeter while slowly sweeping the magnetic field.

Periodic oscillations in the magnetoresistance will occur as a result of the Landau levels passing through the Fermi level E_f. In a degenerate system, which strictly applies in our case,

$$E_f = \frac{(\pi\hbar)^2}{2m_0{}^* m_D{}^*}\left(\frac{3n}{\pi}\right)^{2/3},$$

where $m_D{}^* = m_T{}^* N_v{}^{2/3} K^{1/3}$ is the reduced density-of-states effective mass, N_v is the number of valleys, and $K = m_L{}^*/m_T{}^*$, the mass anisotropy for a given valley. With $E_f/\hbar\omega = \alpha/B$, where $\omega = eB/m_e{}^*$ is the cyclotron frequency, the period, in units of $1/B$, can then be expressed as $1/\alpha$. The value of α is

$$31.4\,(n/N_v)^{2/3} f(K),$$

for B in units of 10^4 gauss and n in units of $10^{18}/\text{cm}^3$.

For a ⟨111⟩ model, oscillations of a single period would be expected for B along a [100] direction because of the single effective mass associated with this direction. For this orientation the experimentally determined value of α is 4.9 ± 0.3 as obtained in Fig. 2(a). The effective-mass ratio K determined from weak-field magnetoresistance is 4.5 ± 0.5 at 300°K and decreases somewhat at lower temperatures, presumably due to an admixture of ionized impurity scattering.[2] Using this value for K, and the expression for $f(K)_{100}$ as given in Table I, eight- and four-valley models yield $\alpha = 3.3 \pm 0.1$ and 5.2 ± 0.1, respectively. Thus a four-valley ellipsoid model is established.

The treatment of transverse magnetoresistance

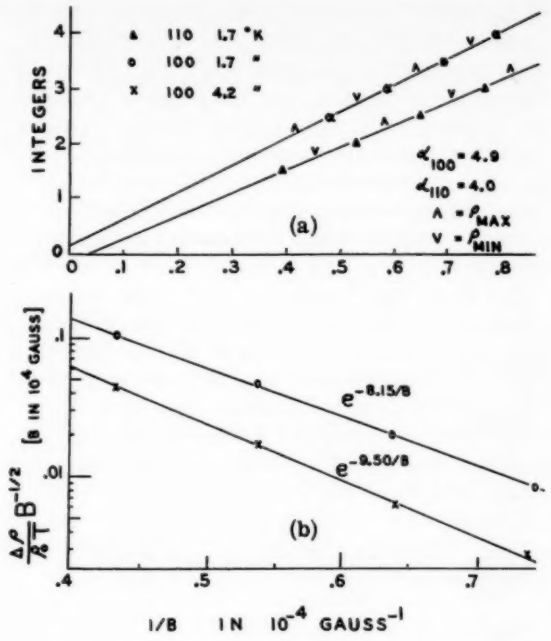

FIG. 2. (a) Nodes of the [001] and [1$\bar{1}$0] oscillations in Fig. 1 plotted at half-integer points for the determination of the periods and the phase shifts. (b) Decay of the B_{001} oscillations vs $1/B$ at 1.7 and 4.2°K for the determination of the damping factors and thus the cyclotron effective mass $(m_e{}^*)_{100}$.

by Adams and Holstein[4] gives the following expression for the oscillatory component for the case of at least several quantum levels and including only thermal broadening:

$$\frac{\rho_{OS}}{\rho} = -C\left(\frac{1}{\hbar\omega E_f}\right)^{1/2} T \sum_{M=1}^{\infty} \frac{(-1)^M \cos(2\pi M E_f/\hbar\omega - \frac{1}{4}\pi)}{M^{1/2} \sinh(2\pi^2 M k T/\hbar\omega)},$$

where ρ is the resistivity in the classical limit

Table I. Values of $m_e{}^*$ and $f(K)$ for two B directions and ellipsoids along the ⟨111⟩ axes.

B	$m_e{}^*$	$f(K)$
[100]	$m_T{}^* K^{1/2}[3/(K+2)]^{1/2}$	$K^{1/6}[3/(K+2)]^{1/2}$
[110]	$m_T{}^* K^{1/2}$	$K^{1/6}$
	$m_T{}^* K^{1/2}[3/(2K+1)]^{1/2}$	$K^{1/6}[3/(2K+1)]^{1/2}$

and ρ_{OS} is the oscillatory component. Our experimental results indicate that the damping is so severe that only the first term in the summation need be considered. This striking attenuation in the amplitudes for decreasing B can be attributed to both thermal broadening and broadening of the Fermi level due to inhomogeneities in the crystal, the latter being the dominant effect. Collision broadening should be very small because of the high mobility.

For B in the [110] direction, two periods would normally be observed. However, because of the damping terms, the component due to the high effective mass will be very small after several periods, leaving predominantly the low-effective-mass oscillations. From the data, plotted in Fig. 2(a), the ratio $\alpha_{110}/\alpha_{100}$ determines a value of K in approximate agreement with the value determined from weak-field magnetoresistance at 300°K. In the [100] case, the phase agrees with that predicted by Adams and Holstein. The phase in the [110] case is somewhat shifted from the predicted value as might be expected from a small admixture of the high-mass period.

The damping term which includes the effect of inhomogeneity and thermal broadening can be written as $\exp[-(\beta_1+\beta_2)/B]$, where $\beta_1 \simeq 200(m_e^*/m_D^*)(\Delta n/n)$ and $\beta_2 = 14.8\, m_e^* T$. The observed damping, $\beta_1 \simeq 7$, indicates a value for $\Delta n/n$ of about 10% which is consistent with the measured inhomogeneity.

To obtain the value of the total damping term [where the effect of inhomogeneity broadening is included in Eq. (1)], $\Delta\rho B^{-1/2}/\rho_0 T$ vs $1/B$ was plotted in Fig. 2(b). ρ in Eq. (1) was taken to be the actual resistivity at a given field, i.e., $\rho \propto \rho_0 B$; however, the actual magnetic field dependence in front of the oscillatory term has only a small effect on the determination of the damping factor. Since the difference in the slope at the two temperatures arises from the change in the value of the β_2 term, an effective mass $m_e^* = 0.035 \pm 0.005$ could be determined. Thus for $K = 4.5$, $m_T^* = 0.025 \pm 0.005$, $m_L^* = 0.12 \pm 0.03$, and $m_D^* = 0.10 \pm 0.02$. Thermoelectric measurements at $T \leq 10$°K have given $m_D^* = 0.08 \pm 0.03$.[2]

More complete results will be published in the future, including studies of longitudinal magnetoresistance and Hall oscillations.

We wish to thank V. J. King of this laboratory for the preparation of the samples.

[1]R. S. Allgaier, Phys. Rev. 112, 828 (1958).
[2]M. R. Ellett, K. F. Cuff, and C. D. Kuglin, Bull. Am. Phys. Soc. 6, 18 (1961).
[3]Y. Kanai, R. N. Nii, and W. Watanabe, J. Phys. Soc. Japan 15, 1717 (1960).
[4]E. N. Adams and T. D. Holstein, J. Phys. Chem. Solids 10, 254 (1959).

TRANSVERSE-EVEN VOLTAGE: A HIGH-FIELD GALVANOMAGNETIC EFFECT ASSOCIATED WITH OPEN ORBITS IN METALS

J. R. Klauder and J. E. Kunzler
Bell Telephone Laboratories, Murray Hill, New Jersey
(Received January 30, 1961)

The magnetoresistance, determined from the voltage measured parallel to the current, represents only one component of the even electric field, the even part of the electric field being that part which is unchanged by a reversal of the magnetic field. The other electric field components lie transverse to the current, and account, for example, for the well-known planar Hall effect. Here, we report observations in copper of such transverse voltages, and demonstrate a significant application of the transverse-even voltage in the determination of open-orbit directions. In addition to providing information about the shape of the Fermi surface, we find that these observations vividly support the concept of open orbits.[1]

When the magnetic field lies in the plane transverse to the current the planar Hall effect vanishes. However, an even voltage usually persists due to the presence of a slight longitudinal misalignment of the Hall contacts to the sample. Such voltages are of one sign because they represent reproductions of the magnetoresistance on a reduced scale, and indeed, they are not true transverse voltages. In contrast, the transverse-even voltages which we have observed in high-purity copper single crystals for high magnetic fields transverse to the current do not scale with the magnetoresistance and characteristically exhibit changes of sign.[2] This new behavior, im-

plicit in the definitive work of Lifshitz and Peschanskii,[3] arises from the existence of a bulk anisotropic magnetoresistance tensor whose principal axes are sensitive to magnetic field orientation because of the presence of open orbits. These new voltages make it possible to determine open-orbit directions with significantly less experimental data than would otherwise be required. In addition, these new voltages are more sensitive to some higher order[4] groups of open orbits than are magnetoresistance data alone. The expected theoretical behavior of these new voltages is discussed under certain simplifying assumptions. Predictions based on these arguments are compared with observed results.

Consider those field directions at high magnetic field strength such that an open Fermi surface leads to a non-negligible number of open orbits whose net direction is along a single direction, say for convenience the x direction. In this case, there is only one dominant even term in the magnetoresistance tensor, $\rho_{xx}=H^2a$. The positive factor a is, to a first approximation, field insensitive, depending rather on the details of the scattering mechanism in a complicated manner. Let $\vec{\Omega}$ be a unit vector in the direction of the open orbits and $\vec{j}$ be the current density; then

$$\vec{E}_0=H^2a\,\vec{\Omega}(\vec{\Omega}\cdot\vec{j}) \tag{1}$$

expresses the general relationship between the open-orbit direction, the current, and $\vec{E}_0$, the component of the electric field due to open orbits. The longitudinal voltage $V_l\equiv\vec{D}_l\cdot\vec{E}_0$ is proportional to the resistivity, while the two transverse-even voltages are defined by $V_{t_1}=\vec{D}_{t_1}\cdot\vec{E}_0$ and $V_{t_2}=\vec{D}_{t_2}\cdot\vec{E}_0$. In these expressions, the $\vec{D}_i$ are three orthogonal vectors, either parallel ($i=l$) or transverse ($i=t_1, t_2$) to the current, whose lengths are proportional to their respective magnetoresistance- or Hall-probe separations. If, as the orientation of the magnetic field is changed, a new set of open orbits is encountered whose net direction is parallel to $\vec{\Omega}'$, then a new set of voltages V_l', V_{t_1}', and V_{t_2}' become significant. Various open-orbit directions may be encountered for a continuous rotation of the magnetic field. For each encounter the sign of V_l will be the same since $V_l\propto(\vec{D}_l\cdot\vec{\Omega})^2$. On the other hand, the uniformity of sign need not be maintained for the transverse voltage since $V_{t_i}\propto(\vec{D}_{t_i}\cdot\vec{\Omega})\times(\vec{\Omega}\cdot\vec{D}_l)$, whose sign depends on the relative orientation of $\vec{\Omega}$; this behavior accounts for the changes of sign of the transverse-even voltage that are observed. As a consistency check on the presence of open orbits whose direction has been ascertained from previous measurements, it suffices to compare the predicted transverse-even voltages $V_{t_1}^{\text{pre}}$ and $V_{t_2}^{\text{pre}}$, where

$$V_{t_i}^{\text{pre}}=V_l(\vec{D}_{t_i}\cdot\vec{\Omega})/(\vec{D}_l\cdot\vec{\Omega}), \tag{2}$$

with the corresponding observed values.

The direction $\vec{\Omega}$ of the open orbits, whose presence is signified by a relatively large value of V_l, is determined by

$$\vec{\Omega}=(\text{normalization})[(V_l/D_l),(V_{t_1}/D_{t_1}),(V_{t_2}/D_{t_2})], \tag{3}$$

as expressed in the "sample" coordinate system. This procedure involves considerably less experimental effort than the previous way in which $\vec{\Omega}$ was determined from magnetoresistance data alone, namely, by tracing out a sequence of points of high magnetoresistance in the plane transverse to $\vec{\Omega}$.[5]

One of the strong points of high-field magnetoresistance data is the information they can give regarding suitable topological models of the Fermi surface through the presence of variously directed sets of open orbits which the Fermi surface must support. For an understanding of the complex metals a qualitative model of the Fermi surface should precede the "pinpointing" of certain surface details. The use of the transverse-even voltages should more readily enable the Fermi surface to be determined. We now briefly discuss some of our transverse-even voltage observations in copper.

Figure 1(a) shows the magnetoresistance observed in copper at 18 kgauss in a transverse rotation about an axis near to the $[5\bar{1}1]$ direction. The peaks of magnetoresistance are proportional to H^2 and occur at orientations of the magnetic field for which a sizable number of unidirectional open orbits exist. In Fig. 2 we represent, in a stereographic projection, the data of Fig. 1(a) idealized to either H^2 behavior, represented by short heavy bars, or to saturation. In addition we show the three inequivalent types of principal magnetoresistance "ridges"—great circles on the unit sphere that have been found by earlier measurements to exhibit an H^2 behavior.[5,6] The interpretation of each magnetoresistance ridge requires the existence of open orbits directed normal to the plane of that ridge; thus, open orbits are directed along ⟨100⟩, ⟨110⟩, and ⟨111⟩ axes. Based on this knowledge of the open-orbit

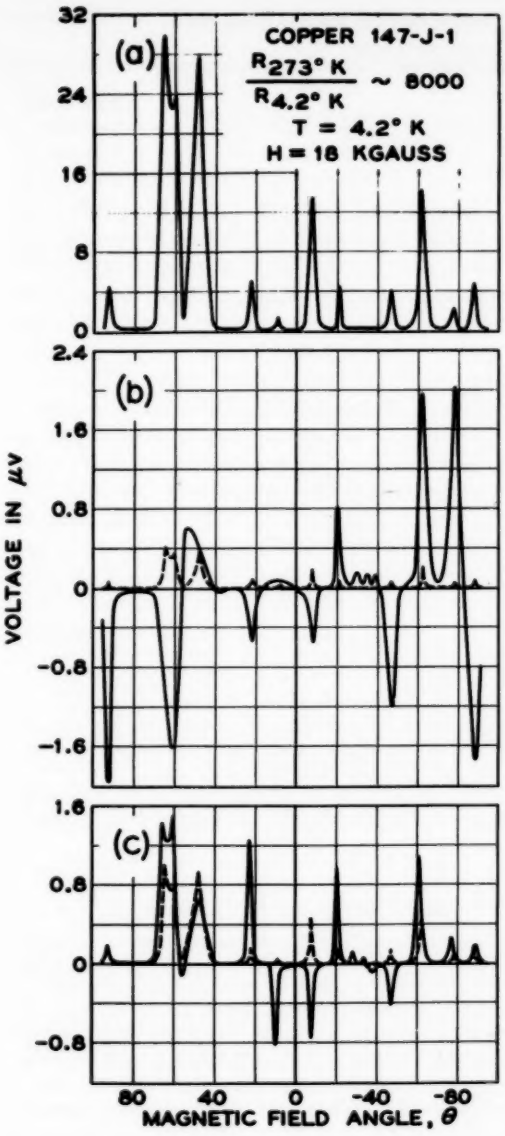

FIG. 1. The longitudinal voltage and the two transverse voltages observed vs angle in a transverse rotation when the current direction is near to a $[5\bar{1}1]$ axis. (a) The longitudinal voltage proportional to the magnetoresistance. (b) and (c) Solid curve: the even part (i.e., less the Hall voltage) of the transverse voltages observed across contacts 2-2′ and 3-3′ as shown in Fig. 2. Dashed curve: that portion, similar to Fig. 1(a), of the solid curve which is due to contact misalignment. The difference of the solid and dashed curves represents the transverse-even voltage present because of the anisotropy of the magnetoresistance tensor due to open orbits.

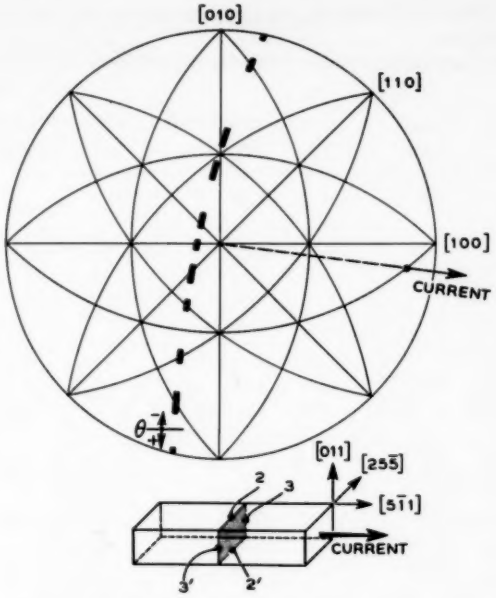

FIG. 2. Stereographic representation of the magnetoresistance data of Fig. 1(a) along with the known contours of H^2 behavior. The sequence of short heavy bars schematically represents the peaks of magnetoresistance observed in the transverse rotation. The great circular lines represent the three inequivalent types of magnetoresistance "ridges" previously observed which indicate the presence of open orbits, along ⟨100⟩, ⟨110⟩, and ⟨111⟩ axes, perpendicular to the ridges of H^2 behavior.

directions for copper, we have calculated the voltage in the two transverse directions that should be observed for each direction of the magnetic field in the transverse plane such that open orbits exist. These results appear in column 3 of Table I.

The solid curves of Figs. 1(b) and 1(c) represent the even part of the observed transverse voltages, while the dashed curves represent that component due to the misalignment voltage, which is a small fixed fraction of Fig. 1(a). In principle, the proportionality constant that relates each dashed curve to Fig. 1(a) can be determined from measurements at zero magnetic field; however, it turned out to be more suitable to determine these factors by a "best fit" to the data. Note the variation in sign; this fact is what first attracted our attention to these voltages. In column 4 of Table I we list the observed transverse voltages at various field angles which,

Table I. Predicted and observed values for the transverse-even voltages at various field angles in a transverse rotation.

Field angle	Open-orbit direction	$V_{t_i}^{pre}$ Predicted[a] voltages (μv)	$V_{t_i}^{obs}$ Observed[a] voltages (μv)	Open-orbit deviation angle
-88°	⟨110⟩	-1.92	-1.82	5°
		0.15	0.03	
-78°	⟨100⟩	2.80	1.97	9°
		0.07	0.20	
-62°	⟨110⟩	2.32	1.77	8°
		0.42	0.62	
-46°	⟨111⟩	-1.26	-1.23	4°
		-0.49	-0.57	
-20°	⟨111⟩	0.91	0.73	6°
		0.83	0.85	
-8°	⟨110⟩	-0.61	-0.77	2°
		-1.27	-1.22	
10°	⟨100⟩	0	0.03	12°
		-1.99	-0.93	
22°	⟨110⟩	-0.35	-0.63	7°
		1.10	1.09	
47°[b]	⟨100⟩, ⟨111⟩	0.5	0.5	...
		-0.31	-0.33	

[a]The top entry in each case is related to Fig. 1(b), while the bottom entry is related to Fig. 1(c).

[b]The top entry of 0.5 μv in this case was assumed to be correct in order to fix a composite open-orbit direction between [100] and [1$\bar{1}$1]. This direction was then utilized to predict the value -0.31 for the bottom entry by Eq. (2).

according to Fig. 1(a), indicate the presence of open orbits so that Eq. (1) has validity.

In column 5 of Table I we list the angle ψ, where $\cos\psi \equiv \vec{\Omega}_{pre} \cdot \vec{\Omega}_{true}$, the deviation between the true open-orbit direction and the direction predicted according to Eq. (3). In nearly every case, the angular deviation ψ does not provide an opportunity for confusion of the open-orbit direction with any other principal crystallographic axis than the correct one. The simple analysis of Eq. (1) ignores additional even terms of lower order in the field; these become significant when $\vec{\Omega} \cdot \vec{j} \approx 0$. The vanishing of $\vec{\Omega} \cdot \vec{j}$ accounts for the absence of any peaks in Fig. 1 when $\theta \simeq -34°$, and its smallness affects the accuracy of the predicted voltages at $\theta = -78°$ and $\theta = 10°$. The transverse voltages appear more sensitive [see field angles between -30° and -40° in Figs. 1(b) and 1(c)] to the "little ridges" which have recently been observed in copper,[5,6] and which may be expected in other metals, whose origins lie in the existence of small bands of higher order open orbits supported by the Fermi surface.

[1]In addition to Hall voltage and magnetoresistance measurements, de Haas-van Alphen observations [e.g., D. Shoenberg, Phil. Mag. 5, 105 (1960)], anomalous skin effect [e.g., A. B. Pippard, Phil. Trans. Roy. Soc. (London) A250, 325 (1957)], cyclotron resonance [e.g., D. N. Langenberg and T. W. Moore, Phys. Rev. Letters 3, 328 (1959)], and magnetoacoustic measurements [e.g., J. D. Gavenda and R. W. Morse, Bull. Am. Phys. Soc. 4, 463 (1959)] give less direct information concerning open orbits.

[2]Similar voltages have been reported by J. Yahia and J. A. Marcus, Phys. Rev. 113, 137 (1959), for gallium, but are not interpreted.

[3]I. Lifshitz and V. Peschanskii, J. Exptl. Theoret. Phys. (U.S.S.R.) 35, 1251 (1958) [translation: Soviet Phys.-JETP 8, 875 (1959)].

[4]J. R. Klauder and J. E. Kunzler, J. Phys. Chem. Solids (to be published).

[5]J. R. Klauder and J. E. Kunzler, Proceedings of the International Conference on the Fermi Surface of Metals, Cooperstown, New York, 1960 (unpublished).

[6]J. E. Kunzler and J. R. Klauder, Bull. Am. Phys. Soc. 5, 150 (1960).

ATTENUATION OF LONGITUDINAL ULTRASONIC VIBRATIONS BY SPIN-PHONON COUPLING IN RUBY

E. B. Tucker
General Electric Research Laboratory, Schenectady, New York
(Received January 30, 1961)

The attenuation of 9.1-kMc/sec longitudinal ultrasonic vibrations due to spin-phonon interaction has been observed in pink ruby. The value of the magnetoelastic coupling constant has been obtained from the experimental value of the attenuation.

Calculations of the "direct process" spin lattice interaction predict that the coupling involved should be quadrupolar in character[1-3] (i.e., through combinations of operators such as S_z^2, $S_xS_z+S_zS_x$, etc.) for non-S-state ions of the iron group such as Cr^{+++}. For longitudinal waves along the z axis, in this case both the trigonal axis of the ruby and the axis of quantization, the interaction may be represented by a perturbation of the form

$$H' = Ge_{zz}S_z^2,$$

where G is the magnetoelastic coupling constant and e_{zz} is the elastic strain amplitude. The resulting transition probability for a spin to absorb a quantum of energy from the phonon field is

$$G^2e_{zz}^2g(\nu)|\langle|S_z^2|\rangle|^2/2\hbar^2.$$

$g(\nu)$ is the shape factor for the spin-lattice interaction, the maximum value having been previously determined as $\simeq 10^{-8}$ sec.[4] $\langle|S_z^2|\rangle$ represents the matrix element of the spin operators between the levels involved. Experimental data for the angular variation of the transition probability, determined using saturation techniques similar to those previously described,[4-6] are given in Fig. 1. Theoretical transition probabilities assuming quadrupole coupling have been computed using the ruby calculations of Chang and Siegman.[7] The experimental data agree quite well with the theoretical curves superposed on a background presumed to be due to transverse components, present by virtue of some longitudinal-transverse mode conversion in the crystal. At $\theta = 0°$ the $\pm 1/2$ (high field 1-3) transition is, as expected, not affected by the phonons while the 1-2 and the other 1-3 transition (both pure $\Delta m = \pm 1$) interact only with transverse waves. It has previously been reported that

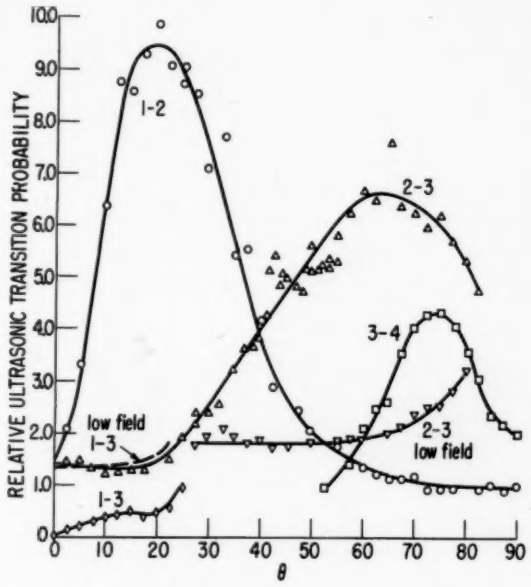

FIG. 1. Angular variation of the ultrasonic transition probability for longitudinal acoustic vibrations along the c axis of pink ruby. The transitions are labeled according to the energy levels involved, with the levels being numbered from the highest (1) to the lowest (4).

Cr^{+++} in ruby obeys the quadrupole selection rules.[8]

The value of the attenuation per centimeter of path is

$$\alpha = G^2g(\nu)|\langle|S_z^2|\rangle|^2nh\nu/(2\hbar^2\rho v^3),$$

where n is the population difference per centimeter between the levels involved, v is the velocity of longitudinal acoustic waves, and ρ is the density of ruby. Since we appear to be justified in taking the theoretical values for $\langle|S_z^2|\rangle$, the determination of a value for G^2 requires an experimental evaluation of α.

The attenuation observation was made using a pulse echo technique similar to that used to determine the attenuation in quartz.[9,10] A double-

cavity arrangement,[5] ultrasonic drive and spectrometer cavities, allowed the amplitude of the absorption signal to be monitored while the echo experiment was in progress. The ultrasonic drive cavity was pulsed at a rate of 10 cps using half-microsecond pulses of 90-watt peak power. A superheterodyne detection system was used to monitor the power from the drive cavity through a 3-db directional coupler. The crystals used were in the form of rods 3 mm in diameter, a $1\frac{3}{4}$-cm length of X-cut quartz and a $1\frac{1}{4}$-cm length of Linde pink ruby. The axis of the ruby rod is 25 minutes from being parallel to the c axis. The ends of both quartz and ruby are optically polished flat, and are parallel to within one minute. The bonding material is indium.

Figure 2 illustrates the echo pattern observed at 1.5°K. The third echo has traversed the ruby rod four times for a total path length of 5 cm in ruby and $3\frac{1}{2}$ cm in quartz. A longer path length in the ruby would be desirable but, for the particular rod lengths used, echo number four and all succeeding echoes are composites of reflections from the bond and from the end of the ruby. No useful conclusions may be drawn from them. The difference in amplitude of the third echo in the top and bottom trace represents the absorption of phonons by the spin system. The amplitude of the third echo averages 20% lower with the magnetic field at the value required for resonance at $\theta = 60°$ on the 2-3 line compared to its amplitude with the magnetic field just off the resonance value. This transition represents the optimum combination of experimental ultrasonic transition probability and Boltzmann factor. The conclusions below are based on a number of observations made on this transition. Attenuations have also been observed for the 1-2 transition at $\theta = 20°$ and for the 3-4 transition at $\theta = 70°$.

FIG. 2. Echo patterns observed: upper trace with the magnetic field adjusted for resonance at $\theta = 60°$ on the 2-3 transition, and lower trace with the magnetic field just off the resonance value. The origins of the echoes are indicated between the traces.

The attenuation observed is 0.2 for the 5-cm path or 0.04 per cm. The corresponding value of G^2 is 1.5×10^{-29} erg^2. If a direct process is assumed for the relaxation process and this value of the coupling constant is assumed to apply to the transverse as well as to the longitudinal waves, the corresponding spin-lattice relaxation time is 0.5 second, assuming Orbach's formula[11]

$$1/T_1 = G^2|\langle|S_z^2|\rangle|^2\omega^2kT/(2\pi\hbar^2\rho v^5),$$

with $T = 4.2$°K and a velocity (the mean of the longitudinal and transverse velocities) of 9×10^5 cm/sec. There are experimental relaxation-time measurements[12,13] which agree quite well with this figure, while others[14,15] are an order of magnitude lower. In any case the experimental relaxation time results do not show the variation with frequency predicted by this formula.

Attenuations were not observable at $\theta = 0°$ for any of the three absorption lines allowed by the microwave selection rules. Theoretically this is what one expects since none of the transitions should be directly affected by a longitudinal wave. The sensitivity in the present experiment is, however, such that it is not reasonable to draw any conclusions concerning the relative proportions of longitudinal and transverse waves from these results for $\theta = 0°$. The value of the attenuation observed for coherent longitudinal waves

should be accurate to better than a factor of two. More accuracy should be obtainable with a judicious choice of rod lengths.

It is a pleasure to acknowledge numerous discussions with Dr. N. S. Shiren and Dr. E. H. Jacobsen, and the loan of the pulser from the latter. T. G. Kazyaka helped take a large part of the data.

[1]J. H. Van Vleck, Phys. Rev. 57, 426 (1940).
[2]R. D. Mattuck and M. W. P. Strandberg, Phys. Rev. Letters 3, 369 (1959).
[3]R. D. Mattuck and M. W. P. Strandberg, Phys. Rev. 119, 1204 (1960).
[4]E. B. Tucker, Bull. Am. Phys. Soc. 5, 157 (1960).
[5]E. H. Jacobsen, N. S. Shiren, and E. B. Tucker, Phys. Rev. Letters 3, 81 (1959).
[6]N. S. Shiren, Bull. Am. Phys. Soc. 5, 343 (1960).
[7]W. S. Chang and A. E. Siegman, Stanford Electronic Laboratory Technical Report No. 156-2, 1958 (unpublished).
[8]N. S. Shiren and E. B. Tucker, Phys. Rev. Letters 6, 105 (1961).
[9]E. H. Jacobsen, Phys. Rev. Letters 2, 249 (1959).
[10]H. E. Bömmel and K. Dransfeld, Phys. Rev. Letters 2, 298 (1959).
[11]See, for example, R. L. Orbach, thesis, University of California, 1960 (unpublished).
[12]R. A. Armstrong and A. Szabo, Can. J. Phys. 38, 1304 (1960).
[13]J. A. Giordmaine and F. Nash, Columbia Radiation Laboratory Quarterly Report, June, 1960 (unpublished), p. 17.
[14]C. Kikuchi, J. Lambe, G. Makhov, and R. W. Terhune, J. Appl. Phys. 30, 1061 (1959).
[15]J. H. Pace, D. F. Sampson, and J. S. Thorp, Phys. Rev. Letters 4, 18 (1960).

ANOMALIES IN THE MAGNETIC SUSCEPTIBILITY AND ELECTRICAL RESISTIVITY OF VANADIUM

Jean-Paul Burger
Laboratoire Pierre-Weiss, Institut de Physique, Strasbourg, France

and

Michael Alan Taylor
Solid State Physics Division, Atomic Energy Research Establishment, Harwell, England
(Received January 30, 1961)

An anomaly in the temperature dependence of the electrical resistivity of vanadium has been reported by several workers.[1-4] The temperature at which this anomaly occurs and its exact form seem to be markedly dependent upon specimen purity. The anomaly has been reported as occurring at the following temperatures: 200°K,[1] 210°K,[2] 190°K,[3] and 245°K.[4] Loomis and Carlson[1] also report anomalies in the following physical properties at similar temperatures: lattice constant, Young's modulus, internal friction, thermal expansion, and intensity of x-ray reflections. Hren and Wayman,[2] however, do not find any discernible deviation from linearity in a plot of Young's modulus against temperature. The mechanism responsible for this behavior is not recognized.

The purpose of this communication is to report a previously undetected anomaly in the temperature dependence of the magnetic susceptibility and its association with the resistivity anomaly in the same specimen. Resistivity data on some vanadium-chromium and vanadium-cobalt alloys are also given.

The susceptibility of vanadium between 20 and 293°K has been discussed by Childs, Gardner, and Penfold.[5] Detailed measurements of the variation of susceptibility with temperature have not been previously reported, although it is known[5,6] that the susceptibility increases slightly with decreasing temperature. The variation of susceptibility with temperature for a specimen of 99.9% purity Van Arkel vanadium kindly supplied by the Batelle Memorial Institute, Columbus, Ohio is given in Fig. 1. The impurities (in wt.%) in the vanadium are as follows: C, 0.005; Si, 0.001; Cr, 0.001; Fe, 0.04; Al, 0.005; Cu, 0.001; H, 0.001; N, 0.008; O, 0.020. The measurements were taken on a Foëx-Forrer translation balance in Strasbourg. The relative error associated with each susceptibility measurement is indicated on the graph. The absolute

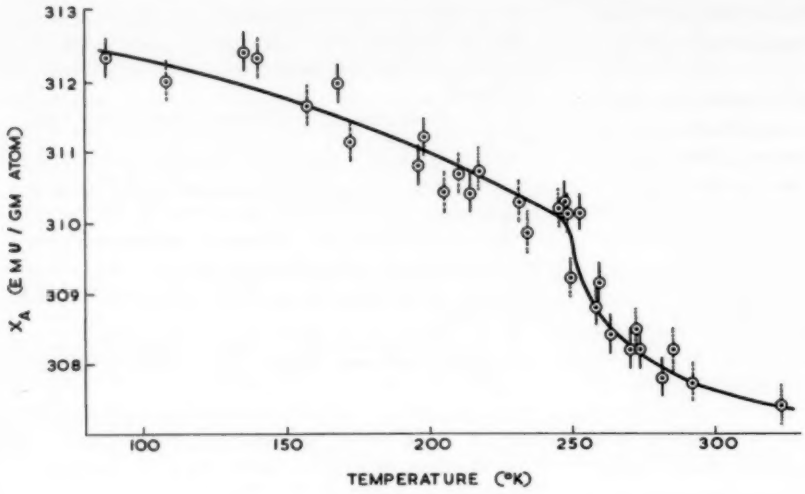

FIG. 1. Variation of susceptibility with temperature.

accuracy of the susceptibility measurements is ±2%; the temperature measurements are accurate to ±2°K. The results of three different runs are indicated (---, ···, —). The susceptibility was independent of magnetic field.

The variation of resistivity with temperature of the same specimen of vanadium is plotted in Fig. 2. The resistivity measurements were taken at Harwell using standard potentiometric techniques. The absolute value of the resistivity is only accurate to ±5%, but the relative accuracies of the measurements are very good, and the measurements are perfectly reproducible. The resistivity at room temperature is 23±1 μohm/cm.

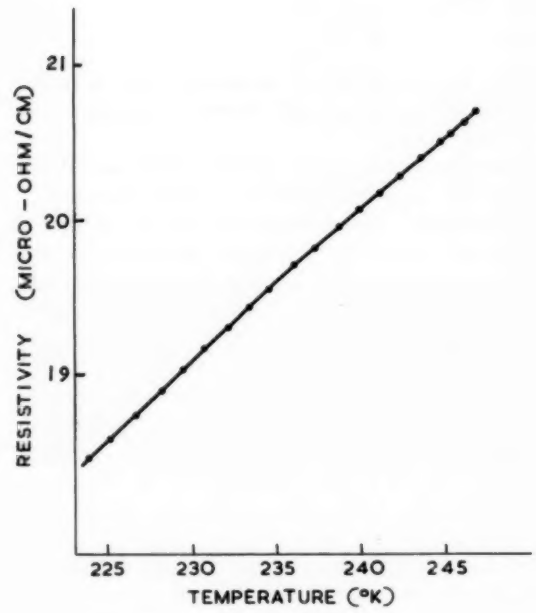

FIG. 2. Variation of resistivity with temperature.

The suggestion by Rostoker and Yamamato[4] that the resistance anomaly is due to a transformation to a body-centered tetragonal phase stable at low temperatures has been shown to be incorrect. No such phase has been detected in low-temperature x-ray investigations by Loomis and Carlson[1] and Hren and Wayman[2] or the present authors. Furthermore no well-defined discontinuity, such as would be expected for a first-order phase change, occurs in the resistivity-temperature plot.

Shull and Wilkinson[7] report that neutron diffraction shows no detectable antiferromagnetic reflection at the (100) position at 20°K and that any moment present must be less than $0.1\mu_B$; this conclusion has also been reached from preliminary neutron diffraction work at Harwell. However, the addition of 2% Cr into solid solution in vanadium lowers the temperature of the resistivity anomaly by 15°C, and the addition of 5% Co by approximately the same amount; this is strongly reminiscent of the results of de Vreis[8] on dilute solutions of transition-metal elements in chromium and seems to indicate that the anomaly is, after all, magnetic in origin and is possibly due to the onset of antiferromagnetism. The fact that no antiferromagnetic moment has yet been observed in vanadium does not prove conclusively that antiferromagnetism does not exist. The time taken by a thermal neutron in

passing from one atom to the next is $\sim 10^{-13}$ sec, whereas the time taken by an electron near the Fermi surface is $\sim 10^{-16}$ sec; therefore if the antiferromagnetism is subjected to some process fluctuating more rapidly than 10^{-13} sec, it is very probable that no (100) peak would be observed.

The problem of the nature of the anomaly is being further investigated.

Thanks are due to Dr. W. E. Gardner (Harwell) for valuable discussions and for providing the alloy specimens, and to Mr. T. E. Baker (Harwell) for carrying out the x-ray investigations.

[1]B. A. Loomis and O. N. Carlson, Iowa State College Report ISC-1037 (unpublished).
[2]J. A. Hren and C. M. Wayman, Trans. Am. Inst. Mining Met. Engrs. 218, 377 (1960).
[3]G. K. White and S. B. Woods, Phil. Trans. Roy. Soc. (London) 251, 273 (1959).
[4]W. Rostoker and A. S. Yamamato, Trans. Am. Soc. Metals 47, 1002 (1955).
[5]B. G. Childs, W. E. Gardner, and J. Penfold, Phil. Mag. 46, 1126 (1959).
[6]C. J. Kreissman and H. B. Callen, Phys. Rev. 94, 837 (1954).
[7]C. G. Shull and M. K. Wilkinson, Revs. Modern Phys. 25, 100 (1953).
[8]G. de Vreis, J. phys. radium 20, 438 (1959).

CAPTURE OF SLOW NEUTRONS BY NUCLEI BOUND IN CRYSTALS*

H. E. Jackson, L. M. Bollinger, and R. E. Coté
Argonne National Laboratory, Argonne, Illinois
(Received December 29, 1960)

The intense interest in the recent discovery[1] of recoilless emission and absorption of γ rays came as a sharp reminder of the classic paper in which Lamb foresaw the comparable effect for neutrons.[2] For neutrons the effect is manifested by the marked influence that crystalline binding of the target nucleus can have on the shape of a resonance. We have undertaken to determine whether the expected distortion in shape can be detected and, if so, to inquire whether it is large enough to give useful information about crystal dynamics.

As was shown by Lamb, it is convenient to consider two sets of conditions under which the shape of a resonance observed with a crystalline target may be expected to depart from the shape that applies to a gas target at the same temperature. First, if the temperature T is not much greater than the Debye temperature θ and if $k\theta$ is much less than the classical recoil energy R, the shape remains that of a Doppler-broadened resonance for a gas target but the effective temperature needed to characterize the magnitude of the Doppler broadening is greater than the physical temperature of the sample. The ratio of the effective temperature T' to the true temperature is given by the equation[3]

$$\frac{T'}{T}=\frac{C_v(\theta/T)}{24}+\frac{3\theta/T}{4[\exp(\theta/T)-1]}+\frac{3}{8}\frac{\theta}{T},$$

where $C_v(\theta/T)$ is the Debye specific heat. Second, under the more extreme conditions $\Gamma \lesssim R < k\theta$ and $T < \theta$, the shape departs significantly from that of a resonance in a gas target at any temperature. The conditions $R < k\theta$ and $T < \theta$ are necessary for a significant fraction of the neutron captures to take place without recoil of the individual target nucleus, and the condition $\Gamma \lesssim R$ is necessary so that the recoilless peak and other structure in the phonon-excitation spectrum of the crystal is not entirely obscured by the natural width of the nuclear level.

In nature there are few materials that satisfy the conditions needed to give a significant departure from the elementary Doppler-broadened shape. Probably the most favorable case is the 6.7-ev resonance in U^{238}. For it $\Gamma = 0.026$ ev and $R = 0.028$ ev so that, if θ is sufficiently high, the predicted effects should be observable. Consequently we have studied the line shapes for capture in two uranium samples, one a metallic foil of normal uranium, for which $k\theta = 0.017$ ev, and the other a sample of U_3O_8, for which $k\theta = 0.038$ ev at liquid nitrogen temperature, according to the available data on specific heats.

The shape of the uranium resonance was determined by transmission measurements with the Argonne fast chopper[4] operated under conditions such that the time-of-flight resolution width was about 0.038 μsec/m (full width at half maximum), a value which corresponds to an energy spread of 0.018 ev at 6.7 ev. Both the metallic foil and the oxide sample were studied at room temperature and at liquid nitrogen temperature, and the foil was studied at the temperature of

liquid helium. For each of these conditions of operation, the neutron transmissions of the sample were measured over the energy range from about 4.5 to 30 ev in a series of several independent runs. The background counting rate was continuously monitored by passing the neutron beam through filters of platinum and silver that were thick enough to remove all timed neutrons in the neighborhood of the resonances at 11.9 and 5.2 ev.

Some of the data obtained are presented in Fig. 1. The resonance shape for the metallic foil at room temperature was compared with the gas-model shape of a Doppler-broadened resonance by curve fitting. Since crystalline binding is not expected to play a significant role for these data, it was not surprising to find a good agreement, as indicated by a χ^2 test, between the experimental and calculated shapes. The small systematic deviation of the data from the curve in the region of high cross section is due in part to the finite resolution of the chopper, which was not included in calculations of the line shapes. The parameters obtained by curve fitting and area analysis of the data are energy $= E_0 = 6.652$ ev, peak cross section $= \sigma_0 = 20\,700 \pm 1200$ barns, $\Gamma = 0.0265 \pm 0.0015$ ev, and $\sigma_0\Gamma = 547 \pm 10$ ev barns. These values are in satisfactory agreement with previously published[5] results.

Having determined reliable values of the resonance parameters from the data for the warm metallic foil, departures of the other data from the simple Doppler-broadened shape may now be detected by comparing the data with the shape calculated from the gas model at the appropriate temperature. Measurements of the metal at $T = 97°K$ are in fair agreement with the gas model. However, in contrast to this, the data on the metal at $T = 4.3°K$ (Fig. 1) and those on the oxide (Fig. 2) at both $T = 297°K$ and $97°K$ are not even

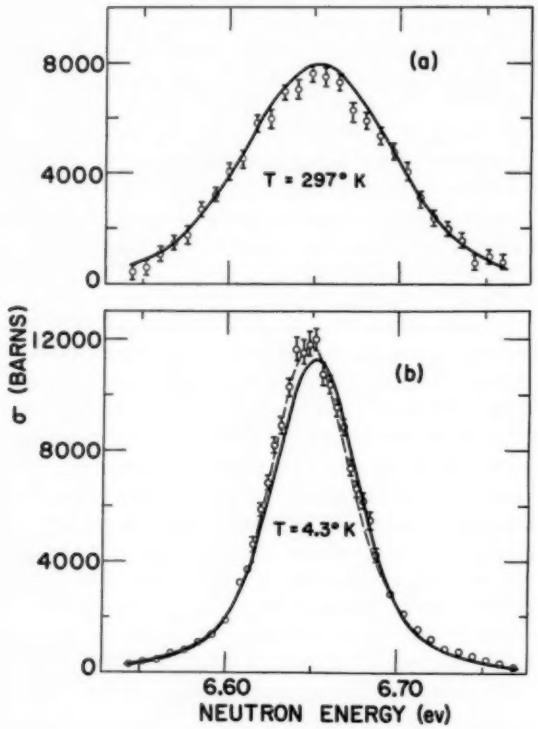

FIG. 1. Total cross-section data for the neutron resonance at 6.65 ev in uranium metal at temperatures of 297°K and 4.3°K. The solid curves are the shapes predicted by the gas model with the physical sample temperature in (a) and with the effective sample temperature (75°K) in (b). The dashed curve of (b) is the shape predicted by a Debye crystal model in which $k\theta = 0.017$ ev.

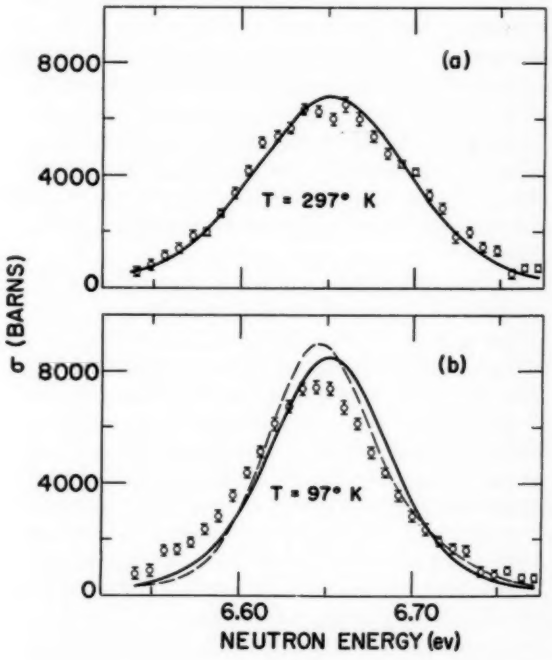

FIG. 2. Total cross-section data for the resonance at 6.65 ev in U_3O_8 at temperatures of 297°K and 97°K. The solid curves are the shapes predicted by the gas model with the effective sample temperatures [334°K in (a) and 181°K in (b)]. The dashed curve of (b) is the shape predicted by a Debye crystal model in which $k\theta = 0.038$ ev.

qualitatively consistent with the gas-model shapes corresponding to the physical temperature. Thus we proceed to compare the data with the gas-model shapes corresponding to the effective temperatures of the samples. This kind of a comparison is made in Figs. 1(b), 2(a), and 2(b), where the solid curves are the Doppler-broadened resonance shapes for effective temperatures 75°, 334°, and 181°K, respectively. The data for the metallic foil at liquid helium temperatures agree with the calculated curve, insofar as the maximum cross section and general shape of the resonance are concerned. However, the energy of the maximum is observed to be displaced toward lower energies. This displacement cannot be an instrumental effect resulting from an instability in the zero time of the neutron time-of-flight system since, on comparing the data for the warm and cold metal foil, the position of the 6.7-ev resonance is observed to move with respect to the other resonances in U^{238} and the resonances in platinum and silver. Thus the displacement of the maximum is believed to be real. It presumably is an indication that an abnormally large fraction of the neutrons are captured with small energy transfers to the crystal lattice. For these events, the incident energy required to excite the nuclear level is less than that required for free nuclei.

Because of its high Debye temperature, we would expect to observe much larger departures from the gas-model shape for a target of U_3O_8. This expectation is fulfilled, as is shown by the data of Figs. 2(a) and 2(b). The line shape at room temperature is adequately described by using the effective-temperature approximation. However, at liquid nitrogen temperature the data show a marked departure from this approximation.

To understand the departure of the observed resonance shape from the effective temperature approximation one must assume a specific model of phonon excitation. Assuming the Debye model to be applicable, we have calculated the shape using the asymptotic expansion of Nelkin and Parks.[6] For the metallic foil the calculated result, as given by the dashed curve of Fig. 1(b), is seen to be in excellent agreement with the experimental data. For the oxide sample, however, the calculated curve is inconsistent with the data of Fig. 2(b). This discrepancy is not surprising since the thermodynamic behavior of U_3O_8 at low temperature indicates that the Debye phonon spectrum may not be appropriate. An analysis is now in progress to attempt to interpret the observed shape of the resonance in terms of a more realistic model.

---

*Work performed under the auspices of the U. S. Atomic Energy Commission.

[1]R. L. Mössbauer, Z. Physik 151, 124 (1958); Naturwissenschaften 45, 538 (1958).

[2]W. E. Lamb, Phys. Rev. 55, 190 (1933).

[3]J. E. Lynn and E. R. Rae, J. Nuclear Energy 4, 418 (1957).

[4]L. M. Bollinger, R. E. Coté, and G. E. Thomas, Proceedings of the Second United Nations International Conference on the Peaceful Uses of Atomic Energy, Geneva, 1958 (United Nations, Geneva, 1958), Vol. 14, p. 239.

[5]L. M. Bollinger, R. E. Coté, D. A. Dahlberg, and G. E. Thomas, Phys. Rev. 105, 661 (1957).

[6]M. S. Nelkin and D. E. Parks, Phys. Rev. 119, 1060 (1960).

ANTISHIELDING OF NUCLEAR ELECTRIC HEXADECAPOLE MOMENTS*

R. M. Sternheimer
Brookhaven National Laboratory, Upton, New York
(Received January 19, 1961)

Up to the present time, evidence for a nuclear electric hexadecapole (16-pole) moment (HDM) seems to have been obtained only in one experiment,[1] probably on account of the fact that the effects of the HDM are masked by the much larger effects of the nuclear quadrupole moment Q. Nevertheless, it is expected that nuclei with spin $I \geq 2$ will have a nonvanishing HDM, and the measurement of its value would obviously constitute a check on any proposed nuclear wave function from which the HDM could be calculated. The purpose of this Letter is to point out that for the case of ions, the effect of the nuclear HDM will be considerably amplified by antishielding effects of the same type as have been calculated[2-4] and observed[5] for nuclear quadrupole moments. An estimate will be made for the antishielding factor η_∞ for the HDM. Here the HDM which is induced in the closed electron shells is written as[6] $H_{\text{ind}} = -\eta_\infty H$, where H is the nuclear HDM. The antishielding effect is due to the excitation of electrons from the closed d shells into higher d states, and similar $nf \to f$ perturbations, produced by the field of the nuclear H. The total HDM of the ion:

$$H_{\text{ion}} = H + H_{\text{ind}} = (1 - \eta_\infty)H, \tag{1}$$

interacts with the fourth-derivative terms of the potential of the lattice, V, evaluated at the nucleus; e.g., $\partial^4 V/\partial z^4$, $\partial^4 V/\partial x^2 \partial z^2$, $\partial^4 V/\partial y^2 \partial z^2$. The average value of the field of H is zero for s and p electrons, so that the antishielding effects will be present only for medium and heavy ions with closed d (and possibly f) shells.

We can define the nuclear HDM as follows:

$$H = \sum_{(p)} \langle r_p{}^4 (35 \cos^4\theta_p - 30 \cos^2\theta_p + 3) \rangle_{m_I = I}, \tag{2}$$

where r_p is the distance of a proton from the center of the nucleus, and the angle θ_p is measured with respect to the z axis (direction of quantization). The expectation value in Eq. (2) is taken over the nuclear wave function with magnetic quantum number $m_I = I$, and the sum extends over all protons in the nucleus. The potential due to H acting on an electron is

$$V_H = eHP_4(\theta)/(8r^5), \tag{3}$$

where r is the distance of the electron from the center of the nucleus, P_4 is the Legendre polynomial, and θ is the angle between the direction of the nuclear spin and the position vector of the electron. The perturbation of the potential energy of the electron in rydberg units is given by

$$v_H = -HP_4(\theta)/(4r^5) \text{ ry}, \tag{4}$$

where r is in units of the Bohr radius a_H, and H is in units $a_H{}^4$.

Upon proceeding in the same manner as in reference 2, one finds that the induced moment density due to the $nd \to d$ and $nf \to f$ (radial) modes of excitation is given by

$$H_{i,\,\text{rad}}(r)dr = Hr^4 \left[\tfrac{80}{63} \sum_n u_0'(nd) u'_{1,H}(nd \to d) + \tfrac{112}{99} \sum_n u_0'(nf) u'_{1,H}(nf \to f) \right], \tag{5}$$

where the sums extend over the closed d and f shells of the core; u_0' is r times the unperturbed (nd or nf) radial wave function, normalized according to $\int_0^\infty u_0'^2 dr = 1$; $u'_{1,H}$ is r times the radial part of the perturbation, and is determined by the equations

$$\left[-\frac{d^2}{dr^2} + \frac{l(l+1)}{r^2} + V_0 - E_0 \right] u'_{1,H}(nl \to l) = u_0'(nl) \left[\frac{1}{r^5} - \left\langle \frac{1}{r^5} \right\rangle_{nl} \right], \tag{6}$$

$$\int_0^\infty u_0'(nl) u'_{1,H}(nl \to l) dr = 0, \tag{7}$$

where V_0 and E_0 are the unperturbed potential and energy eigenvalues for the nl shell, and $\langle 1/r^5 \rangle_{nl}$ is the average value of $1/r^5$ for the wave function $u_0'(nl)$. The coefficients 80/63 and 112/99 in Eq. (5) result from the integration over the angular parts of the wave functions, and the summation over the magnetic substates m. These coefficients $c_H(nl \to l)$ are obtained from

$$c_H(nl \to l) = 8 \sum_{m=-l}^{l} \left[\int_0^\pi |\Theta_l^m|^2 P_4 \sin\theta d\theta \right]^2, \tag{8}$$

where Θ_l^m is the spherical harmonic pertaining to magnetic quantum number m. From Eq. (5), the term $\eta_\infty(nd \to d)$ pertaining to the excitation of the nd shell is given by

$$\eta_\infty(nd \to d) = (80/63)\int_0^\infty u_0'(nd)u'_{1,H}(nd \to d)r^4 dr. \tag{9}$$

An estimate of the order of magnitude of $\eta_\infty(nl \to l)$ can be obtained by using hydrogenic wave functions. This assumes that V_0 and E_0 can be written as $V_0 = -2Z_e/r$ and $E_0 = -Z_e^2/n^2$ (rydberg units), where Z_e is an appropriate effective Z. In this case, the problem of finding the perturbations can be solved exactly, in the same manner as in Eqs. (14)-(20) of reference 3. This calculation has been carried out for $3d \to d$, $4d \to d$, and $4f \to f$, with the following results: $\eta_\infty(3d \to d) = -9274/(63Z_e) = -147.2/Z_e$; $\eta_\infty(4d \to d) = -105\,892/(63Z_e) = -1680.8/Z_e$; and $\eta_\infty(4f \to f) = -24\,524/(495Z_e) = -49.54/Z_e$. In order to evaluate these results, we must obtain the appropriate value of Z_e. Z_e will be a function of the nuclear charge Z; e.g., for $3d \to d$, the value of Z_e will depend on whether the $3d$ shell is the outermost shell of the ion, or whether $4s$, $4p$, and $4d$ shells are also present, so that the $3d$ electrons are essentially internal and see a considerable part of the nuclear potential $-2Z/r$.

For an estimate of Z_e, we may be guided to some extent by the corresponding results obtained for the quadrupole antishielding factor $\gamma_\infty(nl \to l)$. We have found, using hydrogenic wave functions[3]: $\gamma_\infty(2p \to p) = -10.72/Z_e$; $\gamma_\infty(3p \to p) = -40.32/Z_e$; $\gamma_\infty(3d \to d) = -7.77/Z_e$. We can equate these results for $\gamma_\infty(nl \to l)$ with those obtained from Hartree-Fock wave-function calculations[4] to deduce the corresponding values of Z_e. Thus for Na^+, the wave-function result[4] $\gamma_\infty(2p \to p) = -5.16$ leads to $Z_e = 2.08$; for Cl^-, $\gamma_\infty(3p \to p) = -56.5$ gives $Z_e = 0.71$; for Cu^+, $\gamma_\infty(3d \to d) = -8.5$ gives $Z_e = 0.91$. It thus appears that if the np or nd shell considered is the outermost shell of the ion, the effective Z_e is ~1-2. With $Z_e = 1$, one obtains $\eta_\infty(3d \to d) \sim -150$; $\eta_\infty(4d \to d) \sim -1700$; and $\eta_\infty(4f \to f) \sim -50$. The values of $\eta_\infty(nd \to d)$ are very large, and may make it possible to observe the electric hexadecapole moment in quadrupole resonance spectra, using ions in crystals or in polar molecules.

In addition to the strong antishielding effects due to the radial perturbations $nd \to d$ and $nf \to f$, one expects some shielding of the nuclear H due to the angular excitations of the core: $ns \to g$; $np \to f$, $np \to h$; $nd \to g$, and $nd \to i$. This shielding effect can be treated by means of the Thomas-Fermi model of the atom, in the same manner as was done previously[2] for the angular part $Q_{i,\mathrm{ang}}$ of the induced quadrupole moment. One obtains for the density of the induced HDM:

$$H_{i,\mathrm{ang}}(x)dx = \tfrac{1}{6}H(\chi x)^{1/2}dx, \tag{10}$$

where χ and x are the Thomas-Fermi function and variable, respectively; $x = (Z^{1/3}/0.8853)(r/a_H)$. We note that Eq. (10) involves the same function $(\chi x)^{1/2}$ as $Q_{i,\mathrm{ang}}(x)$, the only difference being that the coefficient[2] 3/10 is replaced by 1/6. [In general, the coefficient is given by $(3/2)/(2L+1)$ for a nuclear 2^L-pole moment. Thus if the nucleus had an electric dipole moment D, the density of induced dipole moment would be $\frac{1}{2}D(\chi x)^{1/2}dx$.] In view of Eq. (10), the total induced HDM is given by

$$H_{i,\mathrm{ang}} = \tfrac{1}{6}H\int_0^\infty (\chi x)^{1/2}dx. \tag{11}$$

As was discussed in reference 2, this integral diverges logarithmically at large x, if the Thomas-Fermi function χ (without exchange) is used. However, in the region of $r \lesssim 4a_H$, the Thomas-Fermi result for $Q_{i,\mathrm{ang}}(r)$ agrees reasonably well with that obtained from wave-function calculations, although (as expected) it smoothes over the maxima and minima of $Q_{i,\mathrm{ang}}(r)$ which correspond to the contributions of the various electron shells. From wave-function calculations, we have previously obtained the following values[4,7] of $\gamma_{\infty,\mathrm{ang}}$: 0.60 for Na^+, 1.05 for K^+, 1.4 for Cl^-, and 2.9 for Cs^+. If, following Eq. (11), one assumes that $\eta_{\infty,\mathrm{ang}}/\gamma_{\infty,\mathrm{ang}} = (1/6)/(3/10) = 5/9$, one finds: $\eta_{\infty,\mathrm{ang}} = 0.33$ for Na^+, 0.58 for K^+, 0.78 for Cl^-, and 1.6 for Cs^+. These results show that $\eta_{\infty,\mathrm{ang}}$ is of the order of 1, and is therefore very small compared to the contribution to η_∞ from the radial modes for atoms with closed d shells. Thus for medium and heavy atoms, η_∞ is determined predominantly by the contribution of the radial modes of excitation, which give rise to the antishielding.

The preceding discussion pertains to the case of ions in crystals or in polar molecules, which appear to be the most hopeful possibilities for detecting the nuclear HDM. For the hyperfine structure of valence electrons in neutral atoms, the situation is somewhat different. In this case, the antishielding modes will probably not be nearly as important, since the corresponding per-

turbation of the electron density is located mainly at rather large distances from the nucleus, whereas the interaction with the valence electron takes place very close to the nucleus on account of the $1/r^5$ dependence of the potential V_H. The shielding modes make a relatively large contribution, since the induced density $H_{i,\mathrm{ang}}(x)$ is located somewhat closer to the nucleus. In view of the results of reference 2, one may expect a shielding of the interaction of H with the valence electron of the order of ~10% for light atoms. For heavy atoms, with closed d shells, there may be a net antishielding due to the presence of the radial modes.

Concerning possible experiments with ions in crystals, it seems that the following nuclei offer some good possibilities for observing the nuclear HDM: (1) Zn^{67} ($I=5/2$, $3d^{10}4s^2$); Ge^{73} ($I=9/2$, $3d^{10}4s^24p^2$); (2) In^{113} ($I=9/2$, $4d^{10}5s^25p$); Sb^{121} ($I=5/2$, $4d^{10}5s^25p^3$); Sb^{123} ($I=7/2$); and (3) Bi^{209} ($I=9/2$, $5d^{10}6s^26p^3$). For each nucleus, we have listed the nuclear spin I and the electron configuration of the outer shells. For all cases, the number of electrons outside a closed d shell is small (≤ 5), so that the d shell is essentially external and Z_e is small. The cases listed under (1), (2), and (3) correspond to a newly filled $3d$, $4d$, and $5d$ shell, respectively.

I wish to thank Professor E. M. Purcell for helpful discussions.

---

*Work performed under the auspices of the U. S. Atomic Energy Commission.

[1]T. C. Wang, Phys. Rev. 99, 566 (1955).

[2]R. M. Sternheimer, Phys. Rev. 80, 102 (1950); 84, 244 (1951); 95, 736 (1954); 105, 158 (1957).

[3]H. M. Foley, R. M. Sternheimer, and D. Tycko, Phys. Rev. 93, 734 (1954).

[4]R. M. Sternheimer and H. M. Foley, Phys. Rev. 102, 731 (1956).

[5]See, for example, M. H. Cohen and F. Reif, in Solid State Physics, edited by F. Seitz and D. Turnbull (Academic Press, New York, 1957), Vol. 5, p. 321; T. P. Das and E. L. Hahn, Nuclear Quadrupole Resonance Spectroscopy (Academic Press, New York, 1958).

[6]We use the same convention of signs as for the quadrupole antishielding factor γ_∞; i.e., positive η_∞ corresponds to shielding, while negative η_∞ corresponds to antishielding of the nuclear HDM.

[7]R. M. Sternheimer, Phys. Rev. 115, 1198 (1959).

PION PRODUCTION BRANCHING RATIOS THROUGH THE 900-Mev RESONANCE*

B. A. Munir,† E. Pickup,‡ D. K. Robinson, and E. O. Salant
Brookhaven National Laboratory, Upton, New York
(Received January 30, 1961)

Carruthers and Bethe's discussion[1] of the influence of a π-π interaction on the 900-Mev pion-nucleon resonance involves the experimental branching ratio for the reactions

$$\pi^- + p \rightarrow \pi^- + \pi^+ + n, \qquad (1)$$

and

$$\pi^- + p \rightarrow \pi^- + \pi^0 + p. \qquad (2)$$

In the course of studying pion-proton interactions around 1 Bev, we have measured this ratio for an incident pion energy of 905±2 Mev.

The reactions were produced by magnetically analyzed pions traversing the Brookhaven 20-inch hydrogen bubble chamber, in a field of 12 300 gauss. Events originating in a well-defined central portion of the chamber were measured with digitized microscopes. The events were analyzed with a 704 computer, using the BNL "Tred" program for data reduction and the "Guts" event-fitting program for kinematic identification. The chamber was run so that it was possible to distinguish visually between protons and pions. Of 985 measured two-pronged events, 530 were identified as elastic scattering,[2] 427 as single pion production, and 28 as double production events.

Denoting by n_1 and n_2 the numbers of events of reactions 1 and 2, respectively, the branching ratio r was found to be

$$r = n_1/n_2 = 269/158 = 1.70 \pm 0.17.$$

Values of r from hydrogen bubble chamber observations at energies E near 900 Mev are taken from various authors and are compiled in Table I. It is seen that the measurements are consistent with an approximately constant branching ratio in the 800-1100 Mev energy range.

Early measurements[3] of the cross sections of reactions (1) and (2) produced by 900-Mev pions

Table I. Branching ratios r for incident pion kinetic energies E.

E (Mev)	810[a]	905	960[b]	960[c]	1020[d]	1100[e]
r	2.5 ± 0.4	1.70 ± 0.17	1.25 ± 0.16	1.56 ± 0.19	2.0 ± 0.5	1.67 ± 0.13

[a]L. Baggett, Lawrence Radiation Laboratory Report UCRL-8302, 1958 (unpublished); L. Baggett and B. McCormack, 1958 Annual International Conference on High-Energy Physics at CERN, edited by B. Ferretti (CERN Scientific Information Service, Geneva, 1958), p. 68.
[b]V. Alles-Borelli, S. Bergia, E. P. Ferreira, and P. Waloschek, Nuovo cimento 14, 211 (1959).
[c]E. Pickup, F. Ayer, and E. O. Salant, Phys. Rev. Letters 5, 161 (1960).
[d]I. Derado and N. Schmitz, Phys. Rev. 118, 309 (1960).
[e]E. Pickup, D. K. Robinson, and E. O. Salant (to be published).

in emulsions indicated $r = 0.7 \pm 0.3$. However, the uncertainties involved may not rule out consistency with the bubble-chamber value.

The Carruthers-Bethe model for the reactions (1) and (2), considering the amplitudes a_0, a_1, a_2 of final pion-pion isospin states $t = 0, 1, 2$, predicts that

$$|a_1|^2/|a_0|^2 = (r - \tfrac{1}{2})^{-1},$$

if the $T = 3/2$ state is excluded (so that $a_2 = 0$). By inserting the low emulsion value of r at 900 Mev, a sharp maximum in $|a_1|^2/|a_0|^2$ at that energy was obtained, indicative of a resonant $t = 1$ state. Clearly the new measurement of r at 900 Mev contradicts this conclusion. However, it does not necessarily follow that some other model would not give a dominant $t = 1$ state, even with the branching ratios observed.

We take pleasure in acknowledging our indebtedness to Dr. F. R. Eisler, Dr. N. I. Samios, and Dr. M. Schwartz for preparation of the pion beam, to the BNL Bubble Chamber Group, to the Cosmotron crew, and particularly to our scanners for their unstinting work.

*Work performed under the auspices of the U. S. Atomic Energy Commission.
†On leave of absence from the Florida State University, Tallahassee, Florida.
‡On leave of absence from the National Research Council, Ottawa, Ontario, Canada.
[1]P. Carruthers and H. A. Bethe, Phys. Rev. Letters 4, 536 (1960).
[2]This value is not corrected for scanning losses at small angles.
[3]W. D. Walker, F. Hushfar, and W. D. Shephard, Phys. Rev. 104, 526 (1956).

ELECTRONS IN THE PRIMARY COSMIC RADIATION*

Peter Meyer and Rochus Vogt
Enrico Fermi Institute for Nuclear Studies and Department of Physics,
University of Chicago, Chicago, Illinois
(Received January 16, 1961)

The question of the presence of electrons in the primary cosmic radiation has frequently been discussed in the literature.[1] Attempts to identify such a component have so far been negative. Critchfield, Ney, and Oleksa[2] quote an upper limit of 0.076 (min cm^2 sr)$^{-1}$ for electrons with energies exceeding 1 Bev. In this note we report an experiment which forces us to conclude that there exists a flux of primary electrons which enters the top of the atmosphere.

Three balloon flights were carried out in August and September, 1960 from Fort Churchill, Manitoba which has a calculated geomagnetic cutoff rigidity for vertically incident particles of about 100 Mv (Quenby and Webber[3]). Data were obtained in each flight during the ascent and for approximately 10 hours under 3 to 5 g/cm^2 of residual atmosphere. A cross section through

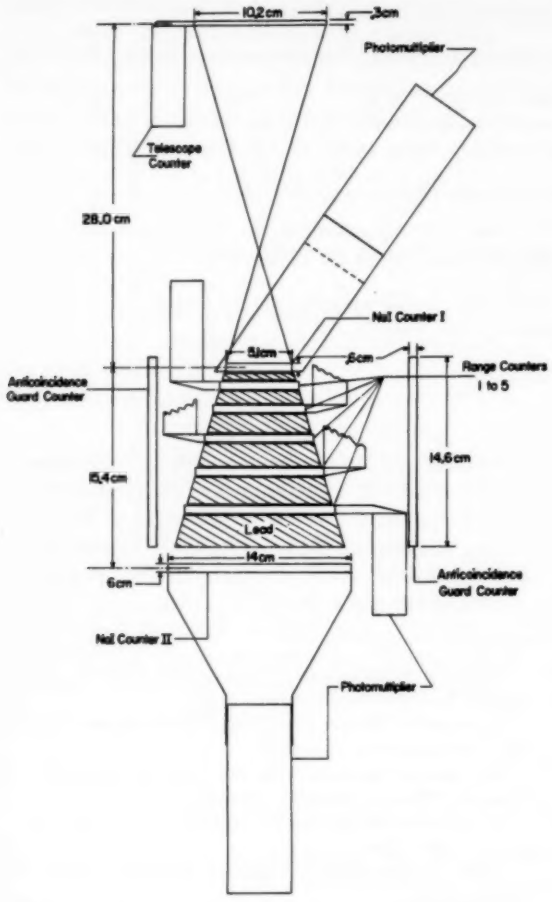

FIG. 1. Cross section of the detector system.

the detector is shown in Fig. 1. The telescope counter and the top NaI counter define the solid angle of acceptance for vertically incident particles. Their range in lead is measured by determining the number of range counters that were triggered in sequence by at least one ionizing particle. The pulse heights from the NaI counters I and II are measured and give the energy loss of particles prior to entering the lead absorber and the energy loss of those particles able to penetrate the entire absorber thickness. This method discriminates against all upward moving charged particles except for those that have minimum energy loss in both NaI counters. The detector system is surrounded on four sides by plastic scintillation counters in anticoincidence.

Protons which come to rest in the lead through ionization are readily identified by their range and the corresponding energy loss in Counter I. In addition to these protons (and α particles) many events are observed which have minimum ionization loss in Counter I but end within the stack of lead absorbers. These events cannot be attributed to protons losing their energy by ionization only, since they would penetrate to counter II, but may be due to (a) high-energy protons making a nuclear collision, (b) mesons, or (c) electrons entering the detector and producing a soft shower in the lead plates.

The altitude dependence of those events is shown in Fig. 2. Near the transition maximum the intensity follows the altitude dependence for secondary electrons (dashed line), while at high altitude it begins to level off or even increase. The dashed line gives the approximate altitude dependence of the secondary electron intensity in air originating from π decay and was arrived at by assuming that the number of π mesons created at any depth in the upper atmosphere is proportional to the flux of high-energy protons present at this depth. It is normalized to the observed intensity at the transition maximum. Obviously, the observed altitude dependence cannot be explained on the basis of secondary electrons.

In Fig. 3 we plot the observed differential range spectrum of the events under discussion at 3 to 4 g/cm^2 atmospheric depth. The dashed line gives

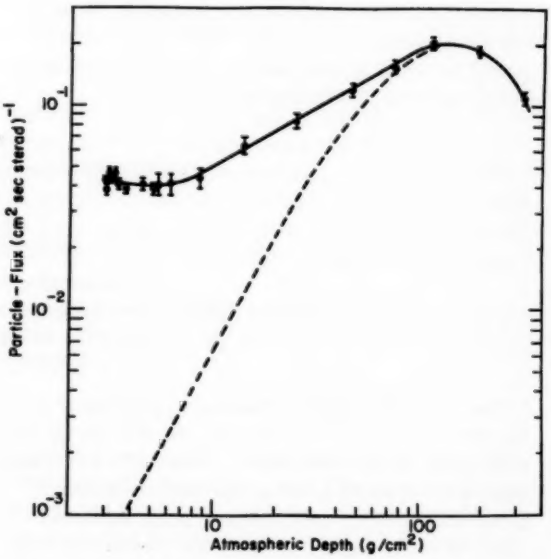

FIG. 2. Intensity versus atmospheric depth. ——— Mimimum-ionizing particles with range between 0 and 120 g/cm^2 of lead (error limits shown are standard deviations). - - - Secondary electrons (computed).

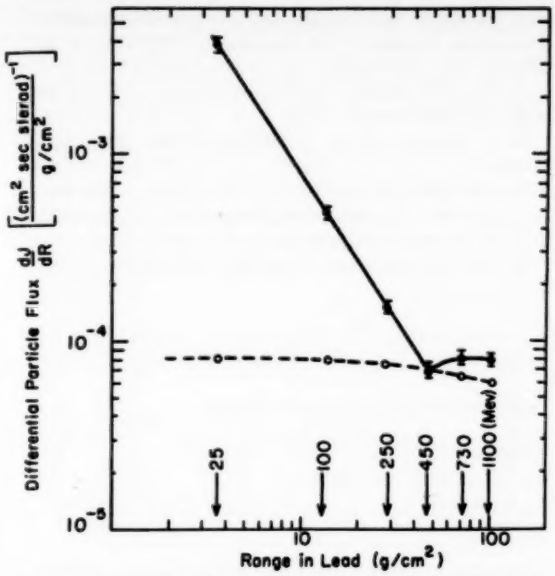

FIG. 3. ——Differential range spectrum of minimum-ionizing particles in lead under 3 to 4 g/cm² of air (error limits are standard deviations). - - - Possible contribution by protons and mesons.

the range spectrum that could be caused by protons and pions under assumptions (a) and (b). A comparison of the curves shows that these particles cannot alone produce the observed range spectrum. Therefore, a substantial fraction of these events is attributed to primary electrons.

We then estimate the energy and flux of the electrons which appear to enter the top of the atmosphere. In particular, we wish to find out whether a portion of the electrons has energies exceeding the geomagnetic cutoff at Fort Churchill for vertical incidence and must, therefore, be of interplanetary or galactic origin. Particles below the geomagnetic cutoff may originate as secondaries from the southern hemisphere. The electrons which enter the lead absorber will in general produce soft showers. We shall have to relate the "range" of the shower to the energy of the incident electron. Greisen and Thom[4] have, for several electron energies, determined the average range in lead at which all ionizing tracks of a shower have disappeared. From their data and Monte Carlo calculations of Wilson[5] we have derived the energy scale in Fig. 3.

We see that primary electrons above the calculated geomagnetic cutoff of 100 Mv are present. All data presented are from a flight on September 8, 1960, at a time of normal solar activity. Measurements on other days lead to the same conclusions.

We here restrict ourselves to deducing a lower and upper limit for the primary electron flux. The lower limit must be derived by subtracting the largest possible contribution of secondary electrons, stopping protons, and mesons. This contribution was obtained by making the extreme assumption that in the range interval with lowest intensity, all the events are due to protons and mesons. The dashed line in Fig. 3, which gives the calculated proton and meson spectrum, is normalized at that point. The difference between the two curves, therefore, represents a lower limit for the electron flux. The possible contribution of secondary electrons to this flux was obtained from Fig. 2 and also subtracted. For reasons not discussed here the effect of upward moving neutrons and γ rays is estimated to be less than 10% of the lower limits.

The upper limits for the electron flux are given by the observed values without subtraction of a possible contribution by protons, mesons, or secondary electrons. This leads to the limits for the vertically incident electron flux that are shown in Table I.

These are preliminary results and detailed calculations of the electron flux and energy spectrum, its time variations, and the implications to the problem of the origin and modulation of cosmic radiation will be published elsewhere.

For many contributions we are indebted to Dr. J. A. Simpson, Dr. E. N. Parker, T. Burdick, R. Weissman, and G. Lentz.

Table I. Flux of vertically incident electrons $(cm^2\ sec\ sr)^{-1}$.

	$25 < E < 100$ (Mev)	$100 < E < 1300$ (Mev)	$E > 1300$ (Mev)
Lower limit	28×10^{-3}	3.5×10^{-3}	0
Upper limit	31×10^{-3}	11×10^{-3}	8×10^{-3}

The series of balloon flights from Fort Churchill was made possible through the cooperation of the National Research Council of Canada.

*This research was supported in part by the Office of Scientific Research, U. S. Air Force, the National Science Foundation, and the Office of Naval Research, U. S. Navy.

[1]See, e.g., V. L. Ginzburg, Progress in Elementary Particles and Cosmic Ray Physics (North Holland Publishing Company, Amsterdam, 1958), Vol. 4, p. 337.

[2]C. L. Critchfield, E. P. Ney, and S. Oleksa, Phys. Rev. 85, 461 (1952).

[3]J. J. Quenby and W. R. Webber, Phil. Mag. 4, 90 (1959).

[4]K. Greisen and H. Thom (unpublished). (We wish to thank these authors for making their results available to us prior to publication.)

[5]R. R. Wilson, Phys. Rev. 86, 261 (1952).

DIRECT Ξ DECAY AND MUONIUM-ANTIMUONIUM TRANSITIONS

Sheldon Lee Glashow
California Institute of Technology, Pasadena, California
(Received January 13, 1961)

It now seems certain that the mass difference between $K_{(1)}^0$ and $K_{(2)}^0$ is quite small ($|\delta m| < 10^{-5}$ ev with 95% confidence[1]). Okun' and Pontecorvo[2] discuss a connection between δm and the existence of $\Delta S = 2$ weak interactions. They show how such an interaction, if as strong as the $\Delta S = 1$ weak interactions, might lead to a mass splitting of the order of electron volts. Indeed, if the $\Delta S = 2$ interaction were absent, a mass difference between the neutral K mesons arises only at second order in the weak interaction and the theoretical estimate, $\delta m^{(2)} \approx 10^{-5}$ ev, agrees with experiment. But suppose L_w (the weak-interaction Lagrangian) includes a $\Delta S = 2$ term (which would permit direct decays of cascade hyperons, i.e., $\Xi^- \to n + \pi^-$, $\Xi^0 \to n + \pi^0$, and $\Xi^0 \to p + \pi^-$). The first order mass splitting, $\delta m^{(1)}$, is equal to twice the matrix element, $M = \langle K^0 | L_w | \bar{K}^0 \rangle$. Noting that $M = \langle \bar{K}^0 | L_w | K^0 \rangle = \langle K^0 | C^{-1} L_w C | \bar{K}^0 \rangle$, where C is the charge-conjugation operator,[3] we find that only the part of the $\Delta S = 2$ coupling which is even under C contributes to $\delta m^{(1)}$. Hence, a $\Delta S = 2$ weak interaction which is odd under C does not lead to a large $K_{(1)}^0$, $K_{(2)}^0$ mass splitting. The small measured value of δm implies nothing about the $\Delta S = 2$, C-odd interaction, but only requires that the $\Delta S = 2$, C-even interaction is no more than 10^{-5} as strong as $\Delta S = 1$ weak interactions.

Assume that a $\Delta S = 2$ interaction odd under C exists with similar strength as ordinary $\Delta S = 1$ weak interactions [the four-Fermion coupling, $G(\bar{\Lambda}\gamma_\lambda n)(\bar{\Lambda}\gamma_\lambda\gamma_5 n) + \text{H.c.}$, is one example[4]]. From CP invariance it follows that any such interaction is also odd under P. Consequently, the effective interaction responsible for direct decay of Ξ into a nucleon and a pion is invariant under space reflection for some assignment of relative Ξ, n parity. The absence of a large δm, although failing to forbid direct Ξ decay, implies that such modes (if they occur at all) cannot display asymmetries (i.e., they "conserve parity"). No direct decays of Ξ have yet been seen. However, existing experimental evidence that direct decay is absent is exceedingly slight.

An identical argument relates the appearance of muonium-antimuonium transitions to the possible existence of interactions permitting $e^- + e^- \to \mu^- + \mu^-$.[5-7] At first sight, looking for spontaneous transitions between muonium and antimuonium seems a more sensitive experiment than the direct search (utilizing, for example, the clashed electron beams soon to be available at Stanford University). But transitions between the 1S states of muonium and antimuonium are generated only by that part of the ($e^- + e^- \to \bar{\mu} + \bar{\mu}$ permitting) interaction which is even under C. To prove this, merely read for $\langle K^0 |$ and $\langle \bar{K}^0 |$ in the first paragraph, the 1S state of muonium and of antimuonium. The interaction $(\bar{\mu}\gamma_\lambda e)(\bar{\mu}\gamma_\lambda\gamma_5 e) + \text{H.c.}$, odd under C, could hardly be detected by looking for the muonium-antimuonium transitions it fails to induce. It could be found directly (by charge-exchange scattering of muons on electrons, or by $e^- + e^- \to \mu^- + \mu^-$), or possibly, by searching for nondegenerate transitions between states of muonium and antimuonium in the presence of external electromagnetic fields.

We wish to thank Professor M. Gell-Mann for

his comments.

[1]F. Muller et al., Phys. Rev. Letters 4, 418 (1960).

[2]L. Okun' and B. Pontecorvo, J. Exptl. Theoret. Phys. (U.S.S.R.) 32, 1587 (1957) [translation: Soviet Phys. -JETP 5, 1297 (1957)].

[3]Actually L_w leads to no violation of either C or P invariance to any order. It is invariant under a charge-conjugation (or parity-reversing) operation which includes a factor of i in the behavior of Λ relative to n. In this note, however, C and P are chosen with customary phases (e.g., real K-meson parity) and L_w is odd under either C or P.

[4]This coupling arises in a partially-symmetric model of weak interactions. S. Glashow (to be published).

[5]B. Pontecorvo, J. Exptl. Theoret. Phys. (U.S.S.R.) 33, 549 (1957) [translation: Soviet Phys. -JETP 6, 429 (1957)].

[6]S. Glashow, Nuovo cimento (to be published).

[7]G. Feinberg and S. Weinberg, invited paper at 1960 Winter Meeting of the American Physical Society at Berkeley, California.

ERRATUM

ANGULAR DISTRIBUTION OF LYMAN-α RADIATION EMITTED BY H(2S) ATOMS IN WEAK ELECTRIC FIELDS, William Lichten [Phys. Rev. Letters 6, 12 (1961)].

On page 12, line 7 from the bottom, read "In the present case $J=\frac{1}{2}$, $m=\pm\frac{1}{2}$, ..."

ABSTRACTS

In this section are printed the abstracts of Articles that have been forwarded to The American Institute of Physics for publication in THE PHYSICAL REVIEW. In quoting information obtained from this section before the appearance of the corresponding Article, reference should be made to "Physical Review (to be published)" rather than to this Journal.

ELECTRICAL BREAKDOWN IN HYDROGEN AT LOW PRESSURES. A. L. Ward, Diamond Ordnance Fuze Laboratories, Washington, D. C., and Eifionydd Jones,* Department of Physics, University of Wales, University College of Swansea, United Kingdom (Received December 13, 1960).

Experimental and theoretical determinations of the static voltage-current characteristics, extending from the region of the Townsend (self-maintained) discharge to the normal glow discharge, have been carried out in hydrogen at low pressures (7-25 mm Hg). The calculations, made on an electronic computer, were based on the distortion of the electric field by space charge, and used the experimentally determined variation of both the primary and secondary Townsend ionization coefficients on the ratio of the field to pressure. Good agreement is obtained between the measured and calculated breakdown and glow voltages, and both the experimental and theoretical curves of the characteristic are of similar shape.

*Now at CERN, European Organization for Nuclear Research, Geneva, Switzerland.

EXPERIMENTAL STUDY OF THE DIAMAGNETISM OF GASEOUS PLASMAS WITH ELECTRON AND NUCLEAR SPIN RESONANCE TECHNIQUES. T. C. Marshall and L. Goldstein, University of Illinois, Urbana, Illinois (Received December 15, 1960).

It has been possible to observe the occurrence of diamagnetism in active discharges by measuring shifts in spin absorption resonance frequencies of foreign substances located near the plasma. Narrow spin electronic resonances in DPPH have been used to show that the magnetization of a gaseous discharge in low-pressure mercury vapor increases linearly with applied magnetic field up to about 40 gauss, where maximization occurs. Observation of the phase change in the Larmor precession of protons in a strong homogeneous field showed that the diamagnetism in a modified Penning ionization gauge discharge increased linearly with power input and decreased approximately as $1/H$. Irradiation of the plasma with high-power microwaves with frequency near the free-electron gyrofrequency resulted in an increase of diamagnetism of the discharge. The discharge magnetic moment ranged from -0.001 to -0.32 erg/cm^3-gauss, depending on experimental conditions. The sensitivity of the nuclear resonance technique is one part in 10^6, and it permits observation of diamagnetism to be deferred until the discharge is over. The theory of plasma diamagnetism is summarized below.

HIGHER RANDOM-PHASE APPROXIMATIONS IN THE MANY-BODY PROBLEM. H. Suhl and N. R. Werthamer, Bell Telephone Laboratories, Murray Hill, New Jersey, and Department of Physics, University of California, Berkeley, California (Received November 4, 1960).

The usual random-phase approximation combined with an equations-of-motion technique for the many-electron problem is extended, yielding many of the known results of series summation methods in a straightforward manner. The method should apply to other types of many-body problems as well.

REFLECTION OF SLOW ELECTRONS FROM TUNGSTEN SINGLE CRYSTALS, CLEAN AND WITH ADSORBED MONOLAYERS. P. Kisliuk, Bell Telephone Laboratories, Murray Hill, New Jersey (Received December 15, 1960).

The reflection of electrons with kinetic energy up to a few electron volts from tungsten single-crystal surfaces is measured both on the clean surface and with adsorbed monolayers of nitrogen and oxygen. For the clean surface, diffraction from the lattice is responsible for a considerable part of the reflection in the thermionic range of energy. The magnitude of the reflection is such as to have a barely measurable effect on experimental tests of the thermionic emission equations. This technique permits continuous recording of the change in work function as gas

is adsorbed, yielding information about the kinetics of chemisorption and the surface dipoles due to the adsorbed gas atoms.

ANHARMONIC ATTENUATION OF LOCALIZED LATTICE VIBRATIONS. P. G. Klemens, Westinghouse Research Laboratories, Pittsburgh, Pennsylvania (Received December 9, 1960).

Lattice modes localized about defects can interchange energy with the continuum of lattice waves by anharmonic interactions. The relaxation time of a localized mode is calculated, taking account of cubic anharmonicities and using perturbation theory analogous to the treatment of three-phonon interactions. At zero temperature the relaxation time is typically of the order of 100 periods, but decreases with increasing temperature.

POTENTIALS IN A CONDUCTOR OF VARYING CROSS SECTION. R. Jaggi, Research Laboratory, International Business Machines Corporation, Zurich, Switzerland (Received November 21, 1960).

A Bernoulli voltage, V_B, proportional to the square of the current I, may be expected in a conductor of varying cross section. Previous experiments to detect V_B are discussed. It is pointed out that in such experiments a Hall voltage, $V_H \propto I^2$, due to the magnetic field of the current I ("eigen-Hall effect" EHE), is superposed on V_B. The ratio V_H/V_B is calculated. Experiments are performed on a bismuth sample of varying cross section. The dependence of the measured voltages upon temperature and cross-sectional area shows that the EHE is dominant over the Bernoulli effect.

EXCHANGE ANISOTROPY IN MIXED MANGANITES WITH THE HAUSMANNITE STRUCTURE. I. S. Jacobs and J. S. Kouvel, General Electric Research Laboratory, Schenectady, New York (Received December 2, 1960).

Magnetic properties are reported of powder compounds isomorphous to hausmannite, but containing partial to nearly complete substitution of diamagnetic Zn^{2+} or Mg^{2+} ions in the tetrahedral sites of Mn_3O_4. X-ray diffraction of these compounds reveals a single phase, whose structure corresponds to a tetragonally distorted spinel. Unidirectional anisotropy is present and is detected by the observation of hysteresis loops displaced along the field axis when the materials are cooled to low temperatures in magnetic fields of several kilo-oersteds. The unidirectional behavior is stable to reverse field pulses of 140 koe. An exchange anisotropy model is proposed involving interactions between ferrimagnetic and nearly antiferromagnetic regions brought about by the random distribution of the diamagnetic ions among the tetrahedral sites and the consequent magnetic inhomogeneity. This model is similar to that proposed for disordered alloy systems. Magnetic viscosity effects are observed which correspond in part to ordinary magnetic viscosity, but which are influenced by the presence of unidirectional anisotropy. The identity of this anisotropy is not impaired by the ordinary viscosity effects. In addition, observations of certain differences in the hysteresis loops measured dynamically and quasi-statically reveal an "extraordinary" viscosity associated with a gradual breakdown of the unidirectional anisotropy.

PARAMAGNETIC RESONANCE OF Gd^{3+} IN Al_2O_3. S. Geschwind and J. P. Remeika, Bell Telephone Laboratories, Murray Hill, New Jersey (Received December 7, 1960).

The electron paramagnetic resonance spectrum of a small impurity of Gd^{3+} in Al_2O_3 has been examined at 24 kMc/sec. The over-all zero-field splitting of the ground state of 1.24 cm^{-1} is the largest so far observed for Gd^{3+}. The analysis of the spectra suggests that the Gd^{3+}, which has twice the ionic radius of aluminum, essentially entered substitutionally for the Al^{3+} (but distorted the environment in such a way as to approach a condition of ninefold oxygen coordination, the symmetry still remaining C_3). The substitution of Gd^{3+} for Al^{3+} whose ionic radius is half as large would indicate that at impurity levels less than 0.02% matching of ionic radii is not an important criterion for incorporation into the lattice.

Although there are two types of Al sites which are physically equivalent, the Gd^{3+} entered selectively into one of these sites. This seemingly paradoxical result is ascribed to the dynamics of the crystal growth. The sites referred to

are actually inequivalent during the growth process as the Gd falls into place and are only equivalent in the grown crystal.

CYCLOTRON RESONANCE IN GERMANIUM. Ralph R. Goodman,* Department of Physics, University of Michigan, Ann Arbor, Michigan (Received April 25, 1960; revised manuscript received January 9, 1961).

Early cyclotron resonance for holes in Ge gave evidence of two resonant peaks associated with the so-called light and heavy holes. Luttinger and Kohn predicted, on the basis of a careful investigation of the theory of degenerate bands, that at low enough temperatures additional peaks should appear. Subsequent experiments confirmed this prediction. In this paper a comparison is made of the cyclotron resonance theory and the experiments of Fletcher, Yaeger, and Merritt. Values of the effective-mass constants which best fit the data are found. Resonant peaks additional to those found by Fletcher, Yaeger, and Merritt are predicted and discussed.

*Now at Colorado State University, Fort Collins, Colorado.

ELECTRON ENERGY BANDS OF ONE-DIMENSIONAL RANDOM ALLOYS. J. S. Faulkner* and J. Korringa, Department of Physics and Astronomy, The Ohio State University, Columbus, Ohio (Received December 5, 1960).

A method for calculating the density of states for an infinite, one-dimensional random alloy is obtained by investigating the asymptotic behavior of the trace of the "transmission" matrix which relates the values taken on by the wave function and its derivative at either end of the crystal. This matrix can be calculated if the potentials of the constituent A and B atoms, V_A and V_B, are given. The equations are first derived for a very general case, and then the results of a calculation for an alloy in which the A and B atoms have equal concentrations is shown for the case that V_A and V_B are δ-function potentials. Certain generalizations of the method for treating other nonperiodic problems are discussed briefly.

*Now with the Department of Physics and the Quantum Theory Project, University of Florida, Gainesville, Florida.

NUCLEAR QUADRUPOLE RESONANCE IN AN ANTIFERROMAGNET. J. C. Burgiel,* V. Jaccarino, and A. L. Schawlow, Bell Telephone Laboratories, Murray Hill, New Jersey (Received December 13, 1960).

Nuclear quadrupole resonance techniques have been used to investigate magnetic interactions in the bromates and iodates of certain $3d$ transition metal ions. In particular, for $Ni(IO_3)_2 \cdot 2H_2O$ there is an abrupt disappearance of the $I^{127}(\pm 3/2 \leftrightarrow \pm 1/2)$ transition at 3.08°K; at lower temperatures there is a large, temperature-dependent splitting. This behavior is attributed to the combined effects of an antiferromagnetic ordering of the Ni^{++} electron spins and a hfs interaction of the nonlocalized Ni^{++} spin magnetization with the I^{127} nuclear magnetic moment. Measurements of the pure quadrupole transition frequencies above, and of their temperature-dependent splittings below, the Néel temperature yield the quadrupole coupling constant, the asymmetry of the electric field gradient (EFG) tensor, the magnitude and orientation of the internal magnetic field relative to the principal axes of the EFG tensor, and the sublattice magnetization as a function of temperature. Qualitative experiments at 1.3°K indicate $T_1^{127} \ll 100$ sec and $T_2^{127} \sim 10^{-6}$ sec. Measurements of the rf and dc magnetic susceptibility have been made and are consistent with these conclusions and, in addition, indicate the sudden onset of a spontaneous ferromagnetic moment as the temperature is lowered below T_n. A possible isotope effect on the T_n of $Ni(IO_3)_2 \cdot 2H_2O$ was looked for but none was found. Cupric iodate and the bromates give no evidence of magnetic ordering above 1.3°K.

*Present address: Department of Physics, Massachusetts Institute of Technology, Cambridge, Massachusetts.

LATTICE THERMAL CONDUCTIVITY OF GERMANIUM-SILICON ALLOY SINGLE CRYSTALS AT LOW TEMPERATURES. Arnold M. Toxen, International Business Machines Research Center, Yorktown, New York (Received December 9, 1960).

Thermal conductivity measurements are reported for five single-crystal Ge-Si specimens containing 0-7.56 atomic percent Si. The measurements were made under steady-state conditions and cover the temperature range 2-50°K.

The experimental results are compared to three theoretical models, those of Berman et al., Callaway, and Klemens; it is found that the data are best fit by Callaway's model. Good agreement between experimental results and theoretical models is obtained by postulating only three sources of phonon scattering in the specimens: three-phonon processes, isotopic point-defect scattering by the germanium and silicon atoms, and boundary scattering. However, evidence is presented that boundary scattering occurs not only at the external surfaces of the specimens, but also at internal surfaces associated with microscale fluctuations of composition of the type reported by Goss, Benson, and Pfann.

ELECTRICAL CONDUCTIVITY OF SINGLE-CRYSTAL CUPROUS OXIDE AT HIGH TEMPERATURES. Robert S. Toth,* Rein Kilkson,† and Dan Trivich, Department of Physics and Department of Chemistry, Wayne State University, Detroit, Michigan (Received November 14, 1960).

The electrical conductivity of single-crystal Cu_2O was measured in the temperature range of 1100° to 500°C in oxygen pressures from 152 mm to 10^{-5} mm of Hg. The $\log\sigma$ vs $\log P(O_2)$ curves were found to be linear between the oxygen pressures of 50 mm and 10^{-2} mm, with an average slope of 0.1420, or approximately 1/7. These curves exhibit a radical change in slope at O_2 pressures below 10^{-2} mm.

The plots of $\log\sigma$ vs $1/T$ at constant oxygen pressure were found to be linear and the activation energies obtained from the slopes of these plots have an average value of 0.65 ev at O_2 pressures between 50 mm and 10^{-2} mm. At O_2 pressures of 10^{-3} mm to 10^{-4} mm, the activation energy increases sharply to a value of 1.05 ev. The activation energy obtained from the measurement of single-crystal Cu_2O in air at temperatures from 1020°C to 1100°C was found to have an average value of 0.767 ev.

An explanation for the physical significance of the activation energies obtained is suggested, and the models proposed to explain the dependence of the electrical conductivity on the O_2 pressure are considered.

*Now at the Physics and Electronics Department, Ford Scientific Laboratory, Dearborn, Michigan.

†Now at the Biophysics Department, Yale University, New Haven, Connecticut.

INFRARED CYCLOTRON RESONANCE IN InSb. E. D. Palik, G. S. Picus,* S. Teitler, and R. F. Wallis, U. S. Naval Research Laboratory, Washington, D. C. (Received November 14, 1960; revised manuscript received January 23, 1961).

Far-infrared cyclotron resonance absorption in n-type InSb has been measured to determine the variation of the conduction electron effective mass with magnetic field. At high magnetic fields the absorption was resolved into a strong line with a weaker satellite line at lower photon energy and a broad, weak absorption at still lower energy. The interpretation of this structure in terms of the conduction band properties of InSb is discussed.

*Now at Hughes Semiconductors Products Division, Newport Beach, California.

NECESSITY AND EXPERIMENTAL CONSISTENCY OF ANTIFERROMAGNETIC GROUND STATE WITHOUT LONG-RANGE ORDER. G. W. Pratt, Jr., Lincoln Laboratory, Massachusetts Institute of Technology, Lexington, Massachusetts (Received December 5, 1960).

A proof is given that long-range order measured as the average value of the z component of sublattice magnetization of an antiferromagnet must be zero in the exact ground state if that state is nondegenerate and the Hamiltonian is invariant under time reversal. The neutron diffraction magnetic cross section is shown not to depend on such a measure of long-range order.

PRESSURE EFFECT ON SUPERCONDUCTING LEAD. M. Garfinkel* and D. E. Mapother, Department of Physics, University of Illinois, Urbana, Illinois (Received November 29, 1960).

Techniques are described for measuring the effect of hydrostatic pressure on the critical field, H_c, of superconducting Pb. Pressures up to 650 atm were applied using solid helium as the pressure fluid. Observations were made from about 7 to 1°K, and values of dH_0/dP, dT_c/dP, and the temperature variation of $(\partial H_c/\partial P)_T$ are reported. From these data the value of $(1/\gamma^*)(d\gamma^*/dP)$ is deduced, where γ^* is the temperature coefficient per unit volume of the normal electronic specific heat. The observed data are accurately represented over the

full range of measurement by the equation $H_C(P,T)=H_0(P)f(t)$, where $t=T/T_C$ and $f(t)$ is independent of pressure. The "similarity principle" requirement, $H_0(P)/T_C(P)=\text{const}$, is shown to be invalid for Pb. The results provide the basis for a discussion of the pressure effects on the net interaction potential, V, of the Bardeen, Cooper, Schrieffer theory and the density of electronic states near the Fermi surface.

*Present address: General Electric Research Laboratory, Schenectady, New York.

GALVANOMAGNETIC PROPERTIES OF n-TYPE $CdAs_2$. A. S. Fischler, International Business Machines Corporation, Poughkeepsie, New York (Received November 21, 1960).

Galvanomagnetic measurements on oriented, single crystals of n-type $CdAs_2$, a noncubic semiconductor, indicate the surfaces of constant energy to be ellipsoids of revolution, located along the symmetry axis of the crystal system. The ratio of electronic mobility is found to be $\mu_\parallel/\mu_\perp \sim 4$, from Hall and resistivity data. Magnetoresistance measurements confirm this conduction band model and indicate the scattering to be due primarily to acoustical lattice modes with some degree of impurity scattering.

PHOTOTHERMAL EFFECT IN SEMICONDUCTORS. W. W. Gärtner, C. B. S. Laboratories, Stamford, Connecticut (Received November 17, 1960; revised manuscript received December 27, 1960).

When a sample of semiconducting material is illuminated, pairs of excess carriers are generated which diffuse through the material according to the density gradients established. Each pair carries an energy approximately equal to the band gap of the material. This energy is deposited where the excess electron recombines with a hole and causes local heating of the lattice. A temperature distribution will therefore be established in the sample which depends on the characteristics of optical absorption and bulk and surface recombination in and on the sample. This establishment of a temperature distribution in a solid by optically excited diffusing and recombining carriers is called the photothermal effect. The paper gives a formulation of the theory governing the photothermal effect, and the case of small temperature elevations in an infinite slab is worked out in detail.

STATISTICAL MECHANICS OF FERROMAGNETISM; SPHERICAL MODEL AS HIGH-DENSITY LIMIT. R. Brout, Laboratory of Atomic and Solid-State Physics and Department of Physics, Cornell University, Ithaca, New York (Received November 15, 1960).

It is shown that there is a class of graphs of the Ising model (or Heisenberg model for $T>T_{\text{Curie}}$) which is comprised of cycle graphs plus some excluded-volume effects which sum to the spherical model. The spherical model, suitably generalized for $T<T_{\text{Curie}}$, was conjectured in a previous work to be the high-density limit of the Ising model, correct to $1/z$. $z^{1/3}$ measures the range of the exchange potential. This is now proved by examining the omitted graphs. The error is shown to be $O(1/z^2)$.

MAGNETIC TORQUE CURVES FOR A SINGLE CRYSTAL OF THULIUM ORTHOFERRITE ($TmFeO_3$). Chinji Juroda, Tomonao Miyadai, Akira Naemura, Nobukazu Niizeki, and Hisao Takata, Electrical Communication Laboratory, Nippon Telegraph and Telephone Public Corporation, Musashino-shi, Tokyo, Japan (Received November 21, 1960).

The magnetic anisotropy of a thulium orthoferrite single crystal was investigated by means of an automatically recording torque-magnetometer in the range between 77 and 300°K. It was found that at room temperature the direction of weak magnetization, σ_0, associated with an antiferromagnetic canted spin arrangement is parallel to the c axis of orthorhombic structure, and that at about 100°K a magnetic transition occurs, where the direction of σ_0 changes from the c axis to the a axis. The transition temperature obtained is the highest among those reported before on other orthoferrites. The torque curves obtained above the transition temperature are similar to those by Sherwood et al. and can be explained by their model. The value of σ_0 is equal to 0.06 μ_B/mole at room temperature. At 77°K below the transition temperature, however, inexplicable torque curves were obtained in the b plane. The curves showed a

small jump at the c axis superimposed on a $\sin 2\theta$ curve with large amplitude. The jump amplitude is almost independent of the applied field in the range of 8500 to 3000 oe. This behavior cannot be explained by Sherwood's model, but it will give information on the interaction between thulium and ferric ions.

GALVANOMAGNETIC EFFECTS IN n-Ge IN THE IMPURITY CONDUCTION RANGE. R. J. Sladek and R. W. Keyes,* Westinghouse Research Laboratories, Pittsburgh, Pennsylvania (Received December 13, 1960).

Measurements of the magnetoresistance and magnetic field dependence of the Hall coefficient of several samples of n-type germanium in the impurity conduction range have been made employing magnetic field strengths up to 28 kgauss. The magnitude and the crystalline anisotropy of the magnetoresistance are interpreted in terms of the changes in the donor wave functions which are produced by the magnetic field. The field dependence of the Hall coefficient is interpreted as a magnetoresistance effect of the conduction band.

*Present address: IBM Research Laboratory, Poughkeepsie, New York.

EFFECT OF CONFIGURATION MIXING AND COVALENCY ON THE ENERGY SPECTRUM OF RUBY. S. Sugano* and M. Peter, Bell Telephone Laboratories, Murray Hill, New Jersey (Received December 1, 1960).

For the purpose of improving the analysis hitherto done of the optical and microwave spectrum of ruby, a calculation has been performed in the strong cubic field scheme, taking into account the effect of configuration mixing of the higher excited t_2^2e states into the t_2^3 states. In the calculation, covalency of the t_2 and e electrons is also introduced in a simplified fashion besides the spin-orbit interaction, trigonal field, and Zeeman energy.

The result shows that configuration mixing and covalency play a very important role in giving zero-field splittings and g values of the t_2^3 states. It is also found that there is not much difference between the degrees of covalency for the t_2 and e electrons, although they are fairly large for both electrons. The best zero-field splitting of the ground state thus obtained is 0.24 cm^{-1} with the correct sign.

*On leave from the Department of Physics, Tokyo University, Tokyo, Japan.

SUPERCONDUCTING TRANSITION TEMPERATURE OF HIGH-PURITY TANTALUM METAL. J. G. C. Milne, Department of Physics, The University of Sheffield, Sheffield, England (Received October 3, 1960).

The superconducting transition temperature of a high-purity sample of tantalum has been measured and a zero-field value of 4.457°K $\pm$ 0.003°K obtained. The ratio of room temperature resistivity ρ_{295} to the residual resistivity $\rho_{4.2}$ gave a measure of the purity of the sample, a value of 250 being obtained. These results compare very well with those of Budnick. The value of (dH_c/dT) near the zero-field transition temperature was -358 oersteds/°K. An approximate theoretical estimate similar to that done by Pippard for tin shows that small amounts of impurity as measured by the residual resistance ratio will give a decrease in transition temperature of about half that observed experimentally.

PHOTOCONDUCTIVITY AND TRAPPING IN SILVER CHLORIDE CRYSTALS. Albert M. Gordon,* Laboratory of Atomic and Solid State Physics and Department of Engineering Physics, Cornell University, Ithaca, New York (Received December 15, 1960).

Photoconductivity and trapping were investigated in pure, cuprous- and nickel-chloride-doped, and darkened silver chloride crystals. The photoconductivity was measured primarily at 88°K. The initial photoresponse increases with rising absorption constant, peaks at wavelengths for which the absorption constant was 3 to 5 cm^{-1}, and falls rapidly to 1/20 to 1/10 of the peak value at wavelengths at which the absorption constant was 50 to 100 cm^{-1}. This decrease in photoresponse at short wavelengths is explained in terms of trapping and recombination through centers in a surface region. The effect of irradiation and the filling of traps was investigated. Values of the schubweg for electrons in the bulk material were obtained from these experiments. The cuprous-chloride-doped samples had a long-wavelength tail on the photoresponse

curve corresponding to the long-wavelength tail observed on the optical absorption.

The photoconductivity does not show any peaks in the infrared. There was, however, a photoresponse with a threshold at approximately 10 000 A in samples irradiated at 88°K and a peak for those irradiated at room temperature. This response was attributed to photoemission from free silver introduced unavoidably during the preparation of the samples. The warming of samples irradiated at 88°K to fill traps produced no measurable thermoluminescence. Electrical warming curves (measurement of current as a function of time during warming) disclosed a number of trapping levels. All samples except the nickel-doped sample showed peaks at 115°K, 140°K, and 180°K related to activation energies of approximately 0.20 ev, 0.28 ev, and 0.45 ev. The nickel-doped sample showed only peaks at 115°K and 180°K. The cuprous-doped samples and the darkened pure sample showed a peak at 160°K corresponding to a thermal activation energy of approximately 0.36 ev. On some samples another peak was visible at 240°K with a thermal activation energy of approximately 0.62 ev. Possible interpretations for these various peaks are discussed.

*Present address: Department of Physiology, University College, London, England.

TEMPERATURE DEPENDENCE OF THE WORK FUNCTION OF METALS (Mo, Ni). George Comşa Adrian Gelberg, and Beatrice Iosifescu, Institute of Atomic Physics, Bucharest, Rumania (Received August 29, 1960; revised manuscript received December 15, 1960).

The temperature coefficient of the work function (TCWF) of polycrystalline Mo and Ni has been measured in the temperature ranges 600-1100°K and 475-1025°K, respectively, using the electron beam method. Special precautions have been taken in order to avoid systematic errors due to the effect of residual gases, of stray magnetic fields, of incorrect temperature measurement, of cathode temperature variations, etc. During determinations made upon Ni surfaces the terrestrial magnetic field has been compensated. Random error sources have been likewise reduced as much as possible. The main results obtained on surfaces outgassed for many thousands of hours at pressures of 1×10^{-9}- 3×10^{-9} torr are

$$\langle(d\psi_{Mo}/dT)\rangle_{av} = (7.84\pm0.07)\times10^{-5}\ \text{ev/°K},$$

$$\langle(d\psi_{Ni}/dT)_{T>\Theta\ Curie}\rangle = (-3.12\pm0.05)\times10^{-5}\ \text{ev/°K}.$$

At the Curie point of Ni, a theoretically expected variation of the TCWF has been observed:

$$\langle(d\psi_{Ni}/dT)_{T<\Theta} - (d\psi_{Ni}/dT)_{T>\Theta}\rangle_{av} = (-0.99\pm0.17)\times10^{-5}\ \text{ev/°K},$$

but no jump of the work function has been found at this point. Special experiments have shown that the results have not been significantly affected by residual gases. A relation between the TCWF of the various facets of these surfaces has been obtained.

SPECIFIC HEAT OF YTTRIUM IRON GARNET FROM 1.5°K TO 4.2°K. Samuel S. Shinozaki,* Department of Physics, University of California, Berkeley, California (Received December 19, 1960).

The specific heats of two samples of yttrium iron garnet have been measured between 1.5 and 4.2°K. The data have been analyzed into lattice- and spin-wave contributions characterized, respectively, by the Debye temperatures $\Theta_1 = 538$°K, $\Theta_2 = 567$°K, and by $D_1 = 0.81\times10^{-28}$ erg cm^2, $D_2 = 0.85\times10^{-28}$ erg cm^2, where D is defined by the dispersion relation for spin waves, $\hbar\omega = Dk^2$.

*Present address: Ford Scientific Laboratory, Dearborn, Michigan.

ELECTRON CAPTURE FROM He($1s^2$) BY PROTONS. Robert A. Mapleton, Geophysics Research Directorate, Air Force Cambridge Research Laboratories, Air Research and Development Command, L. G. Hanscom Field, Bedford, Massachusetts (Received October 20, 1960).

The two equivalent forms of Born's approximation, prior and post, are used to calculate the electron capture cross section for protons incident on He($1s^2$). These cross sections are calculated for capture into eleven different final states in the energy range 12.5 kev to 1 Mev. Although a rather crude wave function, $(Z^3/\pi a_0^3) \times \exp[-(Z/a_0)(r_1+r_2)]$ ($Z = 1.6875$), is used for He, the prior and post total capture cross sec-

tions do not differ by more than 20% over the energy range investigated. Estimates of the sum of the cross sections for capture into all s states of the hydrogen atom for the two residual ions, $He^+(1s)$ and $He^+(2s)$, are obtained from an adaption of the s-state sum rule as given in the paper of Jackson and Schiff. As in this work of Jackson and Schiff, it is found that the s states provide the major contribution to the total capture cross section. The calculated cross sections agree fairly well with the experimental values. The cross section for capture into the state $He^+(1s)+H(1s)$ is roughly 2.5 times larger than the values obtained by Bransden, Dalgarno, and King.

IONIZATION PRODUCED BY ATOMIC COLLISIONS AT kev ENERGIES. III. J. B. Bulman* and A. Russek, University of Connecticut, Storrs, Connecticut (Received December 13, 1960).

The electron evaporation model of the collision-ionization process that occurs when atoms collide at high energies is extended to include atoms with from two to eight electrons in the outer shell. Application of the model to data from collisions of N^+ on Ar and Ne^+ on Ar gives evidence for a resonant electron capture effect taking place in high-energy violent collisions which was heretofore masked by the multiple ionization consequent on such collisions.

*Now at Central Connecticut State College, New Britain, Connecticut.

STRUCTURE IN THE IONIZATION NEAR THRESHOLD OF RARE GASES BY ELECTRON IMPACT. S. N. Foner and B. H. Nall, Applied Physics Laboratory, The Johns Hopkins University, Silver Spring, Maryland (Received August 1, 1960; revised manuscript received January 25, 1961).

Ionization efficiency curves for xenon, krypton, and argon have been studied with an electron energy analyzer. The electron energy distribution was measured and the absolute voltage scale determined in each experiment. The results of these studies (1) favor a linear threshold ionization law over a 1.127 power law, and (2) show that the data cannot be explained simply by ionization processes with onsets at the $^2P_{3/2}$ and $^2P_{1/2}$ ground states of the ion, but can be well fitted by a series of linear processes. The ionization potentials obtained by extrapolating according to a linear threshold law agree with spectroscopic values to within 0.02 ev. New onsets in argon were observed at about 0.64 v and 1.27 v above threshold. The observed structures in the rare gases are not readily explained by auto-ionization and no alternative explanation is offered. The structures observed in these experiments are compared with the results obtained by other "high-resolution" techniques. This comparison is complicated by the disparity in the published data on onset energies, and by the even greater disagreement on the relative probabilities for the various ionization processes. An independent check on consistency of data was made by comparison with "low-resolution" data obtained on a conventional mass spectrometer. The present data are in excellent agreement with the lower resolution data, while some of the other "high-resolution" data are not.

PROTON-HYDROGEN SCATTERING SYSTEM. Marvin H. Mittleman, Lawrence Radiation Laboratory, University of California, Livermore, California (Received August 26, 1960).

The impact parameter treatment of the scattering of protons by hydrogen is derived and is shown to be valid for energies greater than a few volts. A novel treatment of the resultant equations is given which significantly modifies previously obtained results for inelastic scattering and charge-exchange scattering.

SPECTRA INDUCED BY 200-kev PROTON IMPACT ON HELIUM. R. H. Hughes, R. C. Waring,* and C. Y. Fan,† Physics Department, University of Arkansas, Fayetteville, Arkansas (Received November 3, 1960; revised manuscript received January 9, 1961).

Spectra induced by 200-kev proton impact on helium have been observed in the spectral region of λ3500 A to λ6000 A. ^1S states appear to be strongly excited. Absolute cross sections for the direct excitation of the 4 ^1S and 5 ^1S states of neutral helium were determined as well as the simultaneous ionization and excitation cross section for helium into the $n=4$ state of He^+. Of the more intense lines only the 2 ^1P - n ^1S lines and the HeII λ4686 line behaved linearly with pressure within experimental error. Triplet

spectra were observed in which the dominant feature was the $2\,^3P - n\,^3D$ lines. The populations of the $4\,^3D$ and $4\,^1D$ states, in particular, were analyzed as a function of a direct mechanism and collision of the second kind which seem to fit the data fairly well. A very weak Doppler-shifted H_β line was detected. If this is interpreted to be produced by charge exchange, then the cross section for electron capture into the $n=4$ state of hydrogen is estimated to be of the order of 8×10^{-21} cm^2.

*Now at the University of Kansas City, Kansas City, Missouri.

†Now at the Laboratories for Applied Science, University of Chicago, Chicago, Illinois.

VARIATION-PERTURBATION METHOD FOR EXCITED STATES. Oktay Sinanoğlu,* Department of Chemistry and Lawrence Radiation Laboratory, University of California, Berkeley, California (Received July 22, 1960).

The first-order wave function, X_1, in the perturbation method can be obtained by a variational principle instead of summing the usual infinite series with a large continuum contribution. For a ground state or the lowest state of a given symmetry suitable trial functions, $\tilde{X}_1$, are chosen to attain E_2, the second-order contribution to the energy, as a minimum. This method is extended here to any excited state, m. To obtain X_1^m, the expression

$$\tilde{E}_2^{\,m} = \Big\{ 2\langle \Phi_0^{\,m}, (H_1 - E_1^{\,m})\tilde{X}_1^{\,m}\rangle + \langle \tilde{X}_1^{\,m}, (H_0 - E_0^{\,m})\tilde{X}_1^{\,m}\rangle \Big\} \geq E_2^{\,m}$$

is to be minimized with $\tilde{X}_1^m$ in the form

$$\tilde{X}_1^{\,m} = \bar{X}_1^{\,m} + \sum_{k=1}^{m-1} \frac{\Phi_0^{\,k}\langle \Phi_0^{\,k}, H_1 \Phi_0^{\,m}\rangle}{E_0^{\,m} - E_0},$$

and $\bar{X}_1^m$ orthogonal to the known unperturbed functions of the states lower than m. The X_1 gives also the third-order energy.

*Present address: Sterling Chemistry Laboratory, Yale University, New Haven, Connecticut.

PERTURBATION THEORY OF MANY-ELECTRON ATOMS AND MOLECULES. Oktay Sinanoğlu,* Department of Chemistry and Lawrence Radiation Laboratory, University of California, Berkeley, California (Received July 25, 1960).

Perturbation theory with operator techniques is applied to a nondegenerate many-electron system taking the electron repulsions, $\sum_{i>j}^{N} r_{ij}^{-1}$, as the perturbation. The first-order wave function, X_1, is obtained rigorously in terms of the first-order wave functions of independent two-electron systems. The pair functions containing nuclear parameters can be solved for individually by variational or other methods, then used in various atoms or molecules. For example, the Li atom is built up completely from the $(1s)^2\,^1S$, $(1s2s)\,^1S$ and ^3S states of Li^+. The X_1 gives the energy to third order and as an upper limit to the exact E. The E_2 is equal to the sum of complete pair interactions plus many-body terms of two types: (a) "cross polarization" which exists even in no-exchange intermolecular forces, and (b) Fermi correlations.

*Present address: Sterling Chemistry Laboratory, Yale University, New Haven, Connecticut.

APPLICATION OF THE IMPULSE APPROXIMATION TO THE SCATTERING OF ELECTRONS BY ATOMS: I. INELASTIC SCATTERING BY HYDROGEN ATOMS. R. Akerib, Convair, San Diego, California, and S. Borowitz, Physics Department, New York University, New York, New York (Received November 18, 1960).

A calculation of the ionization cross section and the excitation cross section to the $2S$ and $2P$ states of hydrogen atoms by collision with electrons is carried through by the use of an impulse approximation. The results are then compared to the experimental data and to various other theoretical calculations. The cross sections obtained compare favorably with experiment. The calculations carried out by these methods are no more complicated than the usual approximation methods and are easily adaptable for use with more complicated atoms.

ELASTIC SCATTERING AND REACTIONS OF PROTONS ON O^{18}. R. R. Carlson, C. C. Kim,* J. A. Jacobs,† and A. C. L. Barnard,‡ Depart-

ment of Physics and Astronomy, State University of Iowa, Iowa City, Iowa (Received December 14, 1960).

The elastic scattering $O^{18}(p,p)O^{18}$ and the reactions $O^{18}(p,p'\gamma)O^{18}$, $O^{18}(p,\alpha_0)N^{15}$, and $O^{18}(p,\alpha_{1,2}\gamma_{1,2})N^{15}$ were studied using a thin gas target with the State University of Iowa electrostatic generator. Absolute differential cross sections were measured for the two laboratory angles 86.8° and 159.5° in the incident proton energy range 790 to 3550 kev, and angular distributions for α_0 and p were measured at several energies. Relative yield curves of gamma rays were obtained in the same energy range as above. Two F^{19} levels were observed which have not been previously reported and some new decay modes for previously known levels were observed. From consideration of the detailed shape of the elastic-scattering anomalies and the angular distributions, spin and parity assignments were made to some F^{19} levels.

*Now at Physics Department, University of Southern California, Los Angeles, California.

†Now at Physics Department, Virginia Polytechnic Institute, Blacksburg, Virginia.

‡Now at Physics Department, Rice University, Houston, Texas.

GAMMA-GAMMA DIRECTIONAL CORRELATIONS IN Cs^{133}. Atam P. Arya,* Department of Physics, The Pennsylvania State University, University Park, Pennsylvania (Received November 23, 1960).

Directional correlation measurements have been made on the 356−82 kev, 301−82 kev, and 80−82 kev gamma-gamma cascades in Cs^{133} following the decay of 8-year half-life Ba^{133} with a coincidence scintillation spectrometer using NaI detectors. The observed correlation functions are:

$$W(\theta) = 1 + (0.042 \pm 0.005)P_2(\cos\theta) - (0.0041 \pm 0.0038)P_4(\cos\theta),$$

$$W(\theta) = 1 - (0.0257 \pm 0.011)P_2(\cos\theta) - (0.0002 \pm 0.008)P_4(\cos\theta),$$

$$W(\theta) = 1 + (0.0487 \pm 0.017)P_2(\cos\theta) + (0.0011 \pm 0.012)P_4(\cos\theta),$$

respectively, for the three cascades. These gamma-gamma directional correlations were found to be consistent with spin assignments of $7/2^+$, $5/2^+$, $3/2^+$, $3/2^+$, and $1/2^+$ to the levels at the ground state, 82 kev, 162 kev, 383 kev, and 438 kev in Cs^{133}. The probable assignment of the multipolarities for different gamma rays is as follows: The 356-kev gamma ray is pure $E2$. The 82-kev gamma ray is a mixture of $(96.5 \pm 0.5)\%$ $M1$ and $(3.5 \pm 0.5)\%$ $E2$ with $\delta_{82} = -0.190 \pm 0.014$. The 301-kev gamma ray can have one of two possible mixtures: either $\delta_{301} = +0.123 \pm 0.004$ with a mixture of $(98.5 \pm 1.0)\%$ $M1$ and $(1.5 \pm 1.0)\%$ $E2$, or $\delta_{301} = 3.977 \pm 1.02$ with a mixture of $(6 \pm 2)\%$ $M1$ and $(94 \pm 2)\%$ $E2$. The value of $\delta_{301} = -3.977 \pm 1.02$ is more probable. The 80-kev gamma ray is also found to have two possible values of δ_{80}: either $\delta_{80} = +0.468 \pm 0.094$ with a mixture of $(82 \pm 6)\%$ $M1$ and $(18 \pm 6)\%$ $E2$, or $\delta_{80} = +7.0$ with a mixture of $(2.0 \pm 1.5)\%$ $M1$ and $(98.0 \pm 1.5)\%$ $E2$.

*Permanent home address: 3623, Chawri Bazar, Delhi-6, India.

SIMPLE REALISTIC TREATMENT OF NUCLEAR DIRECT-INTERACTION PROCESSES. Ian B. McCarthy* and Derek L. Pursey,† Department of Physics, University of California, Los Angeles, California (Received October 27, 1960; revised manuscript received January 24, 1961).

Physical arguments are used to predict qualitatively the effect on direct-interaction differential cross sections of the distortion of the wave functions of the scattered particle. These qualitative predictions are confirmed by calculations using a simple but fairly realistic model for the wave-function distortion in (α, α') scattering. The model used is based on examination of the properties of optical-model wave functions. Good fits to experimental data are found using the model for (α, α) scattering in the energy range 20-40 Mev for scattering angles less than 90°. Features of direct-interaction processes involving nucleons are interpreted in terms of a focus in the optical-model wave functions for these particles, but detailed calculations are not presented.

*Permanent address: Department of Mathematical Physics, University of Adelaide, Adelaide, S. Australia.

†On leave of absence from University of Edinburgh, Edinburgh, Scotland. Present address: Institute for Advanced Study, Princeton, New Jersey.

DECAY OF K^{42} and Sc^{44}. John D. McCullen* and J. J. Kraushaar, University of Colorado, Boulder, Colorado (Received December 2, 1960).

The low excited states of Ca^{42} and Ca^{44} have been studied in the decay of K^{42} and Sc^{44}, with special emphasis on the observation of weakly populated states. In the K^{42} decay, gamma rays have been seen at 0.31 Mev (1.1%), 0.49 Mev (< 0.1%), 0.60 Mev (0.1%), 0.90 Mev (0.1%), 1.02 Mev (0.1%), 1.52 Mev (100%), 1.92 Mev (0.3%), and 2.42 Mev (0.2%). The coincidence sequence of the transitions has been measured and a level scheme constructed.

In the Sc^{44} decay, gamma rays have been seen with energies and intensities of 0.68 Mev (3.2%), 1.02 Mev (3.1%), 1.12 Mev (4.7%), 1.16 Mev (100%), 1.50 Mev (1.7%), 1.72 Mev (0.8%), 2.28 Mev (0.2%), and 2.69 Mev (0.2%). Coincidence measurements were also taken for this isotope to clarify the cascade sequences, and a level scheme was constructed. A search was made for low-energy conversion electrons ($E < 1$ Mev) in an effort to establish the existence or nonexistence of a low lying 0^+ state in Ca^{44}, whose analog occurs as the second excited 1.84-Mev state in Ca^{42}. No such conversion electrons were seen, either by electron spectrometer studies or by electron-delayed gamma-ray coincidence measurements. An upper limit of 0.05% of the total decay of Sc^{44} was put on the population of such a state.

*Now at Princeton University, Princeton, New Jersey.

INELASTIC SCATTERING OF DEUTERONS FROM THE MAGNESIUM ISOTOPES. A. G. Blair* and E. W. Hamburger,† University of Pittsburgh, Pittsburgh, Pennsylvania (Received December 2, 1960).

Natural and enriched magnesium targets were bombarded with 15-Mev deuterons from the University of Pittsburgh cyclotron. The reaction products were magnetically analyzed and detected by a scintillator or by nuclear emulsions. Angular distributions were obtained for the deuterons inelastically scattered from the Mg^{24} 1.37-, Mg^{25} 1.61-, and Mg^{26} 1.83-Mev states. The results are compared to the predictions of the plane-wave Born-approximation theory and of the inelastic diffraction-scattering model. The curves obtained from the Born approximation give better over-all correspondence with the experimental points. The inelastic diffraction-scattering model, however, allows one to extract directly the effective values of the nuclear deformation parameter β. One obtains $|\beta| = 0.20$, 0.19, and 0.17 for Mg^{24}, Mg^{25}, and Mg^{26}, respectively. The spectra of deuterons inelastically scattered from Mg^{25} and Mg^{26} were also observed, at $\theta_{lab} \approx 12°$, 30°, and 60°. The only large cross sections in Mg^{25} were those for the 1.61-Mev ($7/2^+$) level and for a level near 3.4 Mev. The strength of the reaction to the latter level suggests that it is the $9/2^+$ member of the ground-state rotational band which, in analogy with Al^{25}, should appear at approximately this energy. The results tend to confirm the selection rule that favors collective excitations over single-particle excitation in inelastic scattering. In Mg^{26} strong scattering was observed only from the first two excited states. A previously unreported Mg^{26} state was found at the excitation energy of 3.614 ± 0.020 Mev.

*Now at Los Alamos Scientific Laboratory, Los Alamos, New Mexico.

†Now at Faculdade de Filosofia, Ciências e Letras (Departamento de Física), Universidade de São Paulo, São Paulo, Brazil.

NUCLEAR SPIN OF Ho^{166}. W. J. Childs and L. S. Goodman,* Argonne National Laboratory, Argonne, Illinois (Received December 2, 1960).

The hyperfine structure of Ho^{166} has been examined by means of the atomic-beam magnetic-resonance technique. The atomic ground state appears to be $^4I_{15/2}$, and g_J has the measured value 1.19509 ± 0.00007, in close agreement with the Russell-Saunders value of 6/5. Only one resonance is observed, and its transition frequency for $0.15 \leq H \leq 150$ gauss is proportional to the magnetic field strength to within experimental error. The simplest interpretation is that the nuclear spin is $I = 0$. It is shown that if $I = 1$, the magnetic hyperfine interaction constant a must be less than 5 kc/sec.

*Currently on leave as a Guggenheim Fellow at the University of Heidelberg, Heidelberg, Germany.

(p,d) PICKUP REACTIONS IN LIGHT NUCLEI. E. F. Bennett,* Palmer Physical Laboratory, Princeton University, Princeton, New Jersey (Received June 20, 1960).

Using a thin proportional counter as a velocity

selector in conjunction with a NaI crystal to measure energy, deuterons from proton-induced reactions in some light nuclei were studied. The detection system was capable of presenting an essentially undistorted spectrum of deuterons in the presence of protons of the same energy and considerably more intense. Angular distributions of deuterons from $C^{13}(p,d)C^{12}$, $N^{14}(p,d)N^{13}$, $N^{15}(p,d)N^{14}$, $F^{19}(p,d)F^{18}$, $Mg^{25}(p,d)Mg^{24}$, and $P^{31}(p,d)P^{30}$ were taken. Butler curves were calculated to fit the experimental distributions and level widths extracted.

*Now at Argonne National Laboratory, Argonne, Illinois.

CARBON-13 NEUTRON TOTAL CROSS SECTION. H. O. Cohn, J. K. Bair, and H. B. Willard, Oak Ridge National Laboratory, Oak Ridge, Tennessee (Received December 9, 1960).

The total neutron cross section of carbon-13 was measured for neutron energies from 110 kev to 9 Mev and from 16 Mev to 23 Mev. Four narrow resonances were observed as well as broad resonance structure above 3 Mev. The most probable spin assignments based on the resonance heights and widths are as follows:

$$E_R = 153 \pm 5 \text{ kev}, \quad \Gamma = 13 \text{ kev}, \quad J = 1^+;$$

$$E_R = 1751 \pm 8 \text{ kev}, \quad \Gamma = 20 \text{ kev}, \quad J = 1;$$

$$E_R = 2432 \pm 10 \text{ kev}, \quad \Gamma = 17 \text{ kev}, \quad J = 2;$$

$$E_R = 2454 \pm 10 \text{ kev}, \quad \Gamma = 10 \text{ kev}, \quad J \geq 1.$$

NUCLEAR INTERACTIONS AND MEAN FREE PATHS OF PROTONS, NEUTRONS, AND α PARTICLES AT ENERGIES AROUND 250 Bev/NUCLEON. E. Lohrmann, M. W. Teucher,* and Marcel Schein,† Department of Physics, University of Chicago, Chicago, Illinois (Received November 2, 1960).

Nuclear interactions of protons, neutrons, α particles, and heavier nuclei of average energy 250 Bev/nucleon were studied in nuclear emulsion. The sources of these particles were fragmentations of heavy primary nuclei of the cosmic radiation. Their energy was determined from multiple scattering measurements. The interaction mean free path for protons is 41 ± 10 cm, for α particles 27 ± 7 cm. The mean free path shows no significant change compared with measurements at lower energies. The mean number of shower particles, $\langle N_S \rangle$, depends appreciably on the mass of the target nucleus. Our best estimate for nucleon-nucleon collisions at 250 Bev is $\langle N_S \rangle = 8.8 \pm 1.9$. A detailed comparison of the estimate of the primary energy obtained from the angular distribution of shower particles with the true primary energy is carried out. The angular distribution of the shower particles will, in an individual case, give a quite unreliable value for the primary energy. On the average, the angular distribution method will overestimate the true primary energy by a factor of 1.3 for interactions with a number of heavy prongs $N_h \leq 5$. If $N_h > 5$, the angular distribution will underestimate the true energy in the average by a factor of 1.8. The angular distributions can be transformed into a system in which they are symmetric. This is even true for collisions with heavy target nuclei ($N_h > 5$). The results for alpha-particle and heavy nucleus collisions are quite similar.

The inelasticity for the proton and neutron interactions shows large fluctuations for individual events. It depends weakly on the number of shower particles and on the mass of the target nucleus. Its mean value is 50%. The mean value for the alpha-particle collisions is 22%.

*Now at the Physikalisches Staatsinstitut, University of Hamburg, Hamburg, Germany.
†Deceased.

NUCLEAR INTERACTIONS OF PROTONS, NEUTRONS, AND SHOWER PARTICLES OF VERY HIGH ENERGY IN NUCLEAR EMULSION. A. Barkow,* B. Chamany,† D. M. Haskin, P. L. Jain,‡ E. Lohrmann, M. W. Teucher, ‖ and Marcel Schein,** Department of Physics, University of Chicago, Chicago, Illinois (Received November 28, 1960).

Eighty-four interactions of protons and neutrons were located in a 22-liter stack of nuclear emulsion by tracing back showers of minimum-ionizing particles to their origins. The distribution of the number of shower particles, and the number of heavily ionizing prongs are presented for 57 events with dip angles $< 17°$. The average energy of these events is 3.5×10^{12} ev.

The average number of shower particles emitted in nucleon-nucleon collisions at this energy is 15 ± 5, as estimated from 8 interactions without heavy prongs. The angular distributions of the shower particles are presented for the 57 events. They can be transformed into a system in which the angular distribution is roughly symmetric. This is true even for the collisions with heavy target nuclei ($N_h > 5$). The degree of anisotropy of the angular distributions is in disagreement with a hydrodynamical model of nucleon-nucleus collisions. A lower limit for the collision mean free path of the primary particles of 20 cm in emulsion was obtained. By scanning the forward cone of the primary interactions, 76 secondary interactions of charged and neutral shower particles were found. The distribution of the prong numbers, of the energy, and the characteristics of their angular distribution are presented. The best estimate of the ratio of secondary collisions produced by neutral particles, and the number produced by charged particles, is $N_n/N_{ch} = 0.40 \pm 0.11$. Adding this result to other published data, it is concluded that $30 \pm 6\%$ of the particles produced in collisions having a primary energy of several Tev are not π mesons. A collision mean free path of 41 ± 8 cm was found for the forward-cone shower particles.

*On leave from the Marquette University, Milwaukee, Wisconsin.

†Now with Atomic Energy Commission, Bombay, India.

‡On leave of absence from the University of Buffalo, Buffalo, New York.

‖Present address: Physikalisches Staatsinstitut, University of Hamburg, Hamburg, Germany.

**Deceased.

ANGULAR DISTRIBUTIONS OF SECONDARY PARTICLES PRODUCED IN HIGH-ENERGY NUCLEAR COLLISIONS AND THE TWO-CENTER MODEL OF MULTIPLE MESON PRODUCTION.

J. Gierula,* D. M. Haskin, and E. Lohrmann, Department of Physics, University of Chicago, Chicago, Illinois (Received November 28, 1960).

The angular distributions of shower particles from 54 nuclear interactions of protons and neutrons with energies $> 10^{12}$ ev in a stack of nuclear emulsions are analyzed. The method consists essentially in normalizing the angular distributions of all events in the $x = \log \tan \theta$ scale to the same dispersion σ. One finds a very significant deviation from the normal distribution predicted by hydrodynamical models. The deviation goes in the direction indicated by the two-center model (two maxima in the plot over the x coordinate). The correlation between the separation of the two emitting centers and σ is also in qualitative agreement with the model. The angular distribution in the rest system of the emitting centers is found to be roughly isotropic. The two-center model also offers an explanation for certain characteristic features observed for the angular distribution of events with a small number of shower particles ($n_s \leq 5$). On the basis of this model a coefficient of inelasticity of ≈ 0.2 is obtained for these events.

Interactions characterized by small evaporation ($N_h \leq 5$) and small numbers of shower particles ($n_s \leq 20$) show the characteristic two-maximum shape. The same shape is found for, presumably central, collisions with heavy nuclei in the emulsion ($N_h > 8$, $n_s > 40$). However, the group of collisions with $N_h \leq 5$, $n_s > 20$ does not show the two maxima. The last two observations cannot be explained by the present simple form of the two-center model.

The results of this paper are in good agreement with a similar analysis carried out by Gierula, Miesowicz, and Zielinski.

*On leave of absence from Cosmic Ray Department, Institute of Nuclear Research, Krakow, Poland.

PHENOMENOLOGICAL STUDY OF PION PHOTOPRODUCTION WITH POLARIZED PHOTONS.

G. T. Hoff, Enrico Fermi Institute for Nuclear Studies, University of Chicago, Chicago, Illinois (Received December 6, 1960).

Expressions for the angular distributions and polarizations of pion photoproduction with polarized photon beams are derived from a phenomenological production matrix. The experiments necessary for the complete determination of the multipole amplitudes are discussed in general, and in particular for the case in which only contributions up to p waves in the final state are important. Complete determination requires circularly polarized beams. But if only s and p waves contribute, experiments with linearly polarized beams completely determine the production matrix. The knowledge of these amplitudes would allow the determination of the unknown p-wave scattering phase-shifts (α_{11}, α_{13}, and α_{31}) up to energies of about 300 Mev.

Invariance properties of the angular distributions and polarizations are found and tables are given.

NUCLEAR CAPTURE OF MUONS WITH ELECTRON EMISSION. M. Conversi, L. di Lella, A. Egidi, C. Rubbia,* and M. Toller, Istituto de Fisica dell' Universitâ, Sezione di Roma dell' I. N. F. N., Roma, Italy (Received December 15, 1960).

Two experiments carried out to search for the process of muon capture with electron emission are reported. The second of the two experiments is nearly 200 times more sensitive than earlier attempts to find this capture mode, but no indication is obtained in favor of the latter. In both experiments negative muons are made to stop in copper, where coherent capture is predominant, so that the "capture electrons" should be emitted with an energy spectrum sharply peaked around 100 Mev. For the branching ratio of the process searched for, relative to ordinary muon capture, upper limits of about 5×10^{-5} and 5×10^{-6} are established, respectively, through the first and second experiment.

*Now at CERN, Geneva, Switzerland.

ELASTIC SCATTERING OF NEGATIVE PIONS BY PROTONS AT 230, 290, 370, AND 427 Mev. Lester K. Goodwin, Robert W. Kenney, and Victor Perez-Mendez, Lawrence Radiation Laboratory, University of California, Berkeley, California (Received December 5, 1960).

The elastic differential cross section for the scattering of negative pions by hydrogen was measured at laboratory-system pion kinetic energies of 230, 290, 370, and 427 Mev. The elastically scattered pions were detected by a counter telescope which discriminated against recoil protons and inelastic pions on the basis of range. Differential cross sections were obtained at nine angles for each energy and were fitted by a least-squares program to a series of Legendre polynomials. At the three higher energies, D waves are required to give satisfactory fits to the data. The real parts of the forward-scattering amplitudes calculated from this experiment are in agreement with the predictions of dispersion theory. The results of this experiment, in conjunction with data from other pion-nucleon scattering experiments, support the hypothesis of charge independence at these higher energies.

PROPERTIES OF COSMIC-RAY AIR SHOWERS AT SEA LEVEL. G. W. Clark, J. Earl, W. L. Kraushaar, J. D. Linsley, B. B. Rossi, F. Scherb, and D. W. Scott, Laboratory for Nuclear Science, Massachusetts Institute of Technology, Cambridge, Massachusetts (Received December 13, 1960).

An investigation at sea level of cosmic-ray air showers with sizes from 5×10^5 to over 10^9 particles is described. The core locations, arrival directions, and particle density distributions of several thousand showers whose cores landed within an area of 10^5 m^2 were determined by the techniques of fast-timing and density sampling. The most important results are as follows: (1) The existence of primary particles with energies greater than 10^{18} ev is established by the observation of one shower with more than 10^9 particles; (2) the function

$$f(r) = 0.45(N/R_0^2)\, r^{-0.7}(1+r)^{-3.2},$$

where $r = R/R_0$ and $R_0 = 79$ m, describes the lateral distribution of particles at distances in the range 50 m $< R <$ 400 m and for showers with sizes in the range $5\times10^5 < N < 10^8$; (3) at distances greater than 50 m from the core the density fluctuations in individual showers have a Poisson distribution; (4) the size and zenith-angle distribution can be represented by the formula

$$s(N,x) = s_0(10^6/N)^{\Gamma+1} \exp[-(x - x_0)/\Lambda],$$

where $x = x_0 \cos\theta$, $x_0 = 1040$ g cm^{-2}, $s_0 = (6.6\pm1.0)\times10^{-8}$ cm^{-2} sec^{-1} sr^{-1}, $\Gamma = 1.9\pm0.1$, $\Lambda = (113\pm9)$ g cm^{-2}, $x_0 < x < 1.3x_0$, and $7\times10^5 < N < 7\times10^8$; (5) no evidence is found of anisotropy in the arrival directions or of a break in the energy spectrum of the primaries up to the largest energies observed; (6) assuming a specific model for shower development and taking into account fluctuations in the depth of the first interaction, the integral energy spectrum of the primaries is $J(E) = J_0(10^{15}/E)^{\gamma}$, where $J_0 = (8.1\pm3.1)\times10^{-11}$ cm^{-2} sec^{-1} sr^{-1}, $\gamma = 2.17$, and 3×10^{15} ev $< E < 10^{18}$ ev.

RANGE OF PROTON-ANTIPROTON ANNIHILATION NEAR 1.0 Bev. Osamu Hara,* School of Physics, University of Minnesota, Minneapolis, Minnesota (Received December 9, 1960).

The range of the proton-antiproton annihilation was calculated for antiprotons with energy near 1 Bev. The point is to get the range of pure annihilation interaction, separating the effect of pion production. It was found that the root mean square of this range is given by $(1.19 \pm 0.07) \times 10^{-13}$ cm almost independently of the energy.

*On leave of absence from Nihon University, Tokyo, Japan.

Λ BINDING IN HYPERNUCLEI BY NONLOCAL INTERACTION. G. Rajasekaran and S. N. Biswas, Tata Institute of Fundamental Research, Bombay, India (Received October 21, 1960; revised manuscript received December 27, 1960).

The characteristics of the Λ-*N* interaction at low energy have been obtained assuming that the Λ-*N* potential is nonlocal but separable and similar to that suggested by Yamaguchi in the case of an *N*-*N* potential. The unknown parameters entering in the proposed potential are determined on the basis of the global symmetry hypothesis of the strongly interacting particles. Our model predicts, in agreement with Dalitz and Downs' phenomenological findings of the nature of the Λ-*N* potential based on hyperfragment data, that there is no bound Λ-nucleon system and that the singlet Λ-*N* potential is stronger than the triplet potential, both being attractive. Binding energies of the Λ particle in light hypernuclei based on the present model are, however, much too high compared with the experimental data. It is further pointed out that although the global symmetry hypothesis ($g_{\Lambda\pi} = g_{\Sigma\pi} = g_{N\pi}$) supplemented by the Yamaguchi-type nonlocal Λ-*N* potential is incompatible with the presently existing data, the restricted symmetry ($g_{\Lambda\pi} = g_{\Sigma\pi} \neq g_{N\pi}$) model is certainly admissible.

V - θ COLLISIONS IN THE LEE MODEL. R. D. Amado, Department of Physics, University of Pennsylvania, Philadelphia, Pennsylvania (Received November 16, 1960).

The methods of dispersion theory are used to obtain an exact expression for the *V* - θ elastic scattering amplitude and the amplitude for the production process, $V + \theta \rightarrow N + 2\theta$, in the Lee model.

MAGNETIC MOMENTS OF THE Λ AND Σ HYPERONS. Katsumi Tanaka, Argonne National Laboratory, Argonne, Illinois (Received April 25, 1960; revised manuscript received September 20, 1960).

A relation among the magnetic moments of Σ^+, Σ^0, Σ^-, and Λ is obtained as a consequence of the proposed symmetries of strong interactions, a minimal electromagnetic coupling for the electromagnetic interactions being assumed. The magnetic moments of the Λ and Σ hyperons are calculated with the aid of mass spectral representations in which only the contributions of the bound states are taken into account. The present calculations of these magnetic moments are compared with various other calculations. Remarks are made on the possible experimental values.